UDC 551.513.1:551.510.534:551.509.312"324"

A QUASI-GEOSTROPHIC MODEL OF THE WINTER STRATOSPHERIC CIRCULATION

JOHN H. E. CLARK[1]
Florida State University, Tallahassee, Fla.

ABSTRACT

A six-level quasi-geostrophic model including radiative and photochemical processes in the manner suggested by Lindzen and Goody is run from a state of joint radiative-photochemical equilibrium for midwinter conditions. The spectral method is used to integrate the equations where all dependent variables are represented by a set of spherical harmonics with east-west wave numbers 0, 1, 2, 3, and 6 included. The winter storage of ozone in the polar lower stratosphere is simulated, and the importance of horizontal planetary scale transports and the vertical eddy diffusion of ozone is demonstrated. The rapid dissipation of upper stratospheric temperature disturbances by joint radiative-photochemical relaxation is discussed, and the importance of tropospheric forcing and nonlinear exchanges of kinetic energy between the planetary scale waves is demonstrated. The energetics of downward-propagating spontaneous warmings is discussed. A full-scale warming is triggered by strengthening the north-south lower tropospheric temperature gradient. Its main energy source is found to be a greatly increased forcing of the stratosphere from below.

1. INTRODUCTION

Recent interest in the stratospheric circulation has mainly concentrated on two problems—the ozone cycle and the stratospheric warming. The poor space and time resolution of balloon observations of stratospheric ozone has severely limited the scope of synoptic studies of the ozone budget. By analyzing surface observations of total ozone, Newell (1963) was able to infer indirectly the importance of northward transports of ozone from its equatorial source. In contrast, numerous observational studies of the stratospheric warming exist, for example Scherhag (1952), Finger and Teweles (1964), Hirota (1967*b*), as well as investigations of the energetics of the warming, for example Reed et al. (1963) and Muench (1965).

Attempts to model the stratosphere have been few. Peng (1965) investigated the force summertime circulation by means of a quasi-geostrophic spectral model. Byron-Scott (1967) used a three-level model based on a time-independent form of the vorticity equation following the scale analysis of Burger (1958). Byron-Scott found that the polar store of ozone could be maintained by horizontal northward planetary scale advection. He also demonstrated that high-latitude stratospheric warmings could be intensified by increased forcing from below. His results verified the earlier contention of Craig and Lateef (1962) that the rapid temperature rises associated with warmings were dynamical and not radiative in origin. The most extensive stratospheric model was that of Manabe and Hunt (1968), Hunt and Manabe (1968), and Hunt (1969) who used an 18-level version of the general circulation model of Smagorinsky et al. (1965). The thermal structure of the winter stratosphere was well simulated, and the midlatitude lower stratospheric temperature maximum was associated with the subsiding portion of the two-cell meridional circulation. They also found that the circulation of the upper stratosphere was maintained, in part, by an upward flux of energy from below.

Because of its intense absorption of solar ultraviolet radiation, ozone has far-reaching consequences on both the thermal and dynamical properties of the stratosphere. It follows that a complete understanding of the general circulation of the stratosphere can only go hand in hand with a thorough comprehension of the photochemical formation and advection of ozone by stratospheric motions.

Until recently, the photochemical theory of ozone of Chapman (1930), based on a scheme of reactions involving allotropes of oxygen only, was widely accepted, since the resulting equatorial vertical distribution and total amount in photochemical equilibrium agreed well with observations (Craig 1950). Recently, however, Hunt (1966) questioned the Chapman theory since it yielded unreasonably high total amounts based on new laboratory measurements of certain pertinent reaction coefficients by Benson and Axworthy (1957). Hunt demonstrated that reactions involving water vapor and some of its derivatives must now be included in the scheme to achieve satisfactory results.

A more exacting test of a photochemical theory for ozone is to run a general circulation model that jointly allows for its photochemical production and advection by atmospheric motions. It is significant that the results of Hunt (1969) were not entirely satisfactory, particularly with respect to the polar store of winter ozone, in which both the photochemistry of a moist atmosphere and a dry atmosphere were used in conjunction with Benson-Axworthy rate coefficients. The results of Byron-Scott

[1] Currently postdoctoral fellow at the National Center for Atmospheric Research, Boulder, Colo., sponsored by the National Science Foundation.

(1967), based on reaction coefficients closer to the old ones used by Craig (1950), were somewhat better especially with respect to the polar amount of ozone; although the fairly arbitrary tropospheric forcing of the stratosphere used could have strongly affected the outcome.

As Dütsch (1961) pointed out, recent laboratory measurements of the same reaction coefficients at one temperature can differ by as much as a factor of 20 with the original values used by Craig (1950) lying in this range. Thus until more definitive laboratory measurements are available, it will be difficult to settle on one photochemical theory for ozone. In this experiment, the Chapman photochemical theory along with the original values of reaction coefficients employed by Craig (1950) and other early workers will be used.

As first suggested by Starr (1960) and later verified by Oort (1964), the main source of kinetic energy for the lower stratosphere is not internal energy conversions but forcing of the region by the troposphere. As Oort found, the direction of the eddy-available to eddy-kinetic energy conversion is reversed from what is observed in the troposphere, in the sense that cold air is rising and warm air sinking to create eddy-available energy.

Reed et al. (1963) and Muench (1965) found, however, that the stratosphere can internally create kinetic energy during a stratospheric warming. Many investigators have thus attempted to explain the warming as a manifestation of some type of local hydrodynamic instability. The results have been inconclusive since no sufficient condition for instability has been found that is clearly satisfied by observations. Murray (1960) found the stratosphere to be nearly always baroclinically and barotropically stable. Hirota (1967*a*) found that the polar vortex could become barotropically unstable once it is elongated through external, probably tropospheric, influences.

Charney and Stern (1962) investigated the stability of the winter stratosphere to quasi-geostrophic disturbances in the presence of both lateral and vertical wind shears. They derived a necessary condition for instability that was satisfied by the polar vortex near 60 km. As the lower boundary condition was altered to allow a north-south temperature gradient, they found the condition for instability was relaxed, facilitating the development of unstable disturbances.

The integration of this model will be initiated from a state of joint radiative-photochemical equilibrium, and the spectral method will be used. The object is threefold. The wintertime ozone budget will be investigated in terms of the joint action of photochemistry and three-dimensional advections by stratospheric motions. A thorough examination of the mean energy cycles of the lower and upper stratospheres will be undertaken with particular emphasis on nonlinear interactions between the wave components to be represented. The mechanics of both spontaneous high-latitude warmings and a full-scale warming precipitated by artificially strengthening the latitudinal lower tropospheric temperature gradient will be investigated.[2]

[2] The author is indebted to Richard S. Lindzen (1969) for suggesting this approach to the full-scale warming.

2. THE MODEL

The quasi-geostrophic formulation of the equations of motion will be used in this study. By performing a scale analysis of the full vorticity equation considering the latitudinal as well as longitudinal scale of the dominant planetary scale disturbances, Deland (1965) and Dickinson (1968) demonstrated the validity of this approach. In addition, Craig (1967) found by calculating individual terms of the full vorticity equation from actual data that the local tendency, horizontal advection, and divergence terms were dominant in the stratosphere.

The simplified approach to radiative and photochemical processes suggested by Lindzen and Goody (1965) will be used. They use a Newtonian approximation to infrared cooling that equates the cooling to a linear function of local temperature. Solar absorption by ozone alone is included, and the Chapman photochemical theory is used.

The energetically consistent formulation of the quasi-geostrophic equations by Lorenz (1960), where pressure (p) is the vertical coordinate, follows:

$$\frac{\partial}{\partial t}\nabla^2\psi=-J(\psi,\nabla^2\psi+f)-\nabla\cdot\left(f\nabla\frac{\partial X}{\partial p}\right)+g^2\mu\frac{\partial}{\partial p}\left(\rho\frac{\partial}{\partial p}\nabla^2\psi\right), \quad (1)$$

$$c_p p_0^{-\kappa}\nabla^2\theta=-\nabla\cdot\frac{\partial}{\partial p^\kappa}(f\nabla\psi), \quad (2)$$

$$\frac{\partial\theta}{\partial t}=-J(\psi,\theta)-\left(\frac{\partial\theta}{\partial p}\right)_s\nabla^2X+\left(\frac{p_0}{p}\right)^\kappa\frac{Q}{c_p}, \quad (3)$$

and

$$\frac{\partial\tau}{\partial t}=-J(\psi,\tau)-\left(\frac{\partial\tau}{\partial p}\right)_s\nabla^2X+2q_2\frac{n_2}{n_m}-2q_3\frac{k_{13}}{k_{12}n_2}\tau^2+g^2\rho K_\tau\frac{\partial}{\partial p}\left(\rho\frac{\partial\tau}{\partial p}\right) \quad (4)$$

where

ω=vertical velocity=∇^2X,
ψ=stream function,
t=time,
J=Jacobian operator,
f=Coriolis parameter,
ρ=density,
μ=vertical dynamic eddy-viscosity coefficient,
g=980 cm sec^{-2},
κ=2/7,
τ=ozone number mixing ratio,
θ=potential temperature,
Q=rate of radiative heating per unit mass of air,
c_p=specific heat of air at constant pressure,
p_0=reference pressure (1000 mb),
K_τ=vertical eddy-diffusion coefficient for ozone,
n_3,n_2,n_m=number density of ozone, oxygen, and air molecules, respectively,
k_{12},k_{13}=reaction coefficients (Lindzen and Goody 1965), and
q_2,q_3=number of quanta absorbed per unit time per unit volume by oxygen, ozone divided by n_2, n_3, respectively.

Equation (1) is the vorticity equation, and equation (2) is a generalized thermal wind equation (Lorenz 1960). According to Lindzen and Goody (1965), the radiative heating Q in the thermodynamic equation (3) is given as

$$Q/c_p=\eta'\tau-aT+b \tag{5}$$

where

$$\eta'=\frac{hn_m}{\rho c_p}\int \alpha_3 I_{o\nu}\nu \exp(-\alpha_2 x_2-\alpha_3 x_3)d\nu,$$

a,b=known constants,
h=Planck's constant,
T=temperature,
$I_{o\nu}$=photon flux outside the atmosphere at frequency ν,
α_2,α_3=absorption cross sections of oxygen and ozone, respectively, and
x_2,x_3=number of molecules of O_2 and O_3 between the point in question and the sun.

In equations (3) and (4), standard values of the lapse rates of potential temperature and ozone mixing ratio denoted by the subscript s are used at each pressure level. By the use of geostrophic winds in the horizontal advection terms and constant lapse rates at each pressure, the only advective effects that will alter the zonally averaged temperature or ozone amount will be horizontal eddy advection and vertical advection by the mean meridional circulation.

The coupling of radiative and photochemical effects in this model is achieved through the dependence on ozone amount of solar heating and the important temperature dependence of the ratio k_{13}/k_{12} given by

$$\frac{k_{13}}{k_{12}}=Ee^{-D/T} \tag{6}$$

where the constants E and D are determined from laboratory measurements.

The initial equilibrium state is found by setting the net radiative heating and photochemical production of ozone in equations (3) and (4), respectively, to zero and solving for τ_e and θ_e, where the subscript e stands for an equilibrium value. The equilibrium stream function, ψ_e, can then be found from equation (2). Letting $\psi=\psi_e+\psi'$, etc., and rewriting equations (1), (3), and (4) in terms of the departures from equilibrium but dropping the primes, we get

$$\frac{\partial}{\partial t}\nabla^2\psi=-J(\psi_e+\psi,\nabla^2(\psi_e+\psi)+f)-\nabla\cdot\left(f\nabla\frac{\partial X}{\partial p}\right)+g^2\mu\frac{\partial}{\partial p}\left(\rho\frac{\partial}{\partial p}\nabla^2(\psi_e+\psi)\right), \tag{7}$$

$$\frac{\partial\theta}{\partial t}=-J(\psi_e+\psi,\theta_e+\theta)-\nabla^2 X\left(\frac{\partial\theta}{\partial p}\right)_s+\eta\tau-a\theta, \tag{8}$$

and

$$\frac{\partial\tau}{\partial t}=-J(\psi_e+\psi,\tau_e+\tau)-\nabla^2 X\left(\frac{\partial\tau}{\partial p}\right)_s-C\theta-B\tau+g^2\rho K_\tau\frac{\partial}{\partial p}\left(\rho\frac{\partial(\tau_e+\tau)}{\partial p}\right) \tag{9}$$

where $\eta=(p_0/p)^\kappa\eta'$.

In the ozone equation (9), only the first-order linear terms in the Taylor expansion of the full photochemical source terms about the equilibrium state have been kept. The expressions for B and C are derived in Lindzen and Goody (1965).

Since motions with time scales much longer than the diurnal period will only be considered, the factors η, B, and C will be considered functions of height and latitude only. They will be multiplied by one-half to account for the alternation between day and night. A constant solar declination of 20° S. was assumed; and η, B, and C were calculated once and for all from the initial equilibrium state.

The spectral method will be used to integrate the equations. It is particularly well suited to problems where only a small number of waves is to be investigated. Teweles (1963) and Perry (1967) have shown that the most active stratospheric waves are those on the planetary scale with east-west wave numbers 1, 2, and 3. Bryan (1959) applied the method to a two-level quasi-geostrophic model. The only stratospheric spectral model has been that of Peng (1965).

One advantage of the method is that the spectral equations always maintain the same energy invariants as the original equations. No general proof of this fact exists, but Platzman (1960) demonstrated it in the case of the barotropic vorticity equation.

Since disturbances whose scales are comparable to the earth's radius are to be considered, a spherical geometry will be used. All dependent variables will be expanded in terms of complex spherical harmonics defined as

$$Y_n^m(\phi,\lambda)=P_n^m(\phi)e^{im\lambda}, \tag{10}$$

where ϕ is latitude and λ longitude. P_n^m is a Legendre polynomial of order m and degree n defined as

$$P_n^m(\phi)=\frac{(2n)!}{2^n n!}\left(\frac{2n+1}{(n-m)!(n+m)!}\right)^{1/2}(1-\sin^2\phi)^{m/2}\times\frac{d^{m+n}}{d\sin\phi^{m+n}}(\sin^2\phi-1)^n. \tag{11}$$

These polynomials are normalized over a hemisphere. For complex harmonics, m can be negative, and $|m|$ is the east-west wave number. The difference $n-|m|$ is a measure of the north-south wave number.

The planetary scale waves of east-west wave numbers 1, 2, and 3 will be represented. Since the stratosphere is to such a large extent driven by the troposphere (Oort 1964), it is imperative that this effect be modeled as precisely as possible. Rather than specify conditions at the tropopause from actual data, this experiment will include the troposphere as well as the stratosphere. As Saltzman and Teweles (1964) have shown, the baroclinically active tropospheric waves transfer significant amounts of energy up the scale to the longer waves through nonlinear interactions. Accordingly, wave number 6 will be added to the spectrum. Teweles (1963) demonstrated using real data that the latitudinal variation of amplitude of the various Fourier components of northern hemispheric

geopotential at 500 and 50 mb for January 1958 usually consisted of a single maximum or minimum near 60° N. Thus it seems appropriate to consider, for each east-west wave number, only the first few modes with lowest values of $n-|m|$. We have no guarantee, however, that the neglected higher modes do not play a significant role in the dynamics especially of the troposphere.

Only harmonics that are symmetric across the Equator, $n-|m|$ even, will be considered. For a midwinter situation, this is obviously quite an over-simplification and could have detrimental effects on the outcome of the experiment, especially in the Tropics. Since the wind field is symmetric, the stream function in terms of which the wind is expressed as a gradient must be antisymmetric. Such a representation avoids the problem of a singularity arising in the thermal wind equation (2) because of the vanishing of f at the Equator. The following set of harmonics will represent θ, τ, and X:

$$\{Y_0^0, Y_2^0, Y_4^0, Y_6^0, Y_1^1, Y_1^{-1}, Y_3^1, Y_3^{-1}, Y_2^2, Y_2^{-2}, Y_4^2, Y_4^{-2}, Y_3^3, Y_3^{-3}, Y_5^3, Y_5^{-3}, Y_6^6, Y_6^{-6}, Y_8^6, Y_8^{-6}\}, \quad (12)$$

while ψ will be represented by

$$\{Y_1^0, Y_3^0, Y_5^0, Y_2^1, Y_2^{-1}, Y_4^1, Y_4^{-1}, Y_3^2, Y_3^{-2}, Y_5^2, Y_5^{-2}, Y_4^3, Y_4^{-3}, Y_6^3, Y_6^{-3}, Y_7^6, Y_7^{-6}, Y_9^6, Y_9^{-6}\}. \quad (13)$$

The harmonics Y_n^m are complex, and thus the spectral amplitudes, for example ψ_n^m, are complex. To ensure that the fields are real, one can easily show that

$$\psi_n^{-m}=(-1)^m\overline{\psi_n^m}, \quad (14)$$

where the bar denotes complex conjugate.

There is little point in following through the tedious but straightforward derivation of the spectral equations. A fairly extensive literature exists on the spectral method, and the reader is referred to Peng (1965), whose approach was quite similar to the present, or to a complete development of this model in Clark (1969). The basic theory on the use of spherical harmonics appears in Silberman (1954).

Figure 1 shows the arrangement of layers and the levels at which each variable is defined. The stratosphere is represented by four layers, the troposphere by two. For the upper boundary condition at $p=0$, the vertical velocity ω was set equal to zero. Topographic and Ekman layer effects were allowed for at the lower boundary.

Muench (1965) presented evidence of long waves originating near the ground and propagating considerable distances into the stratosphere. Topographic effects are believed to be important in exciting such features (Saltzman 1965). Orographically induced vertical velocities were calculated according to

$$\omega_A=-g\rho_1 J(\psi_2,h), \quad (15)$$

where ρ_1 is the density at 1000 mb and ψ_2 is the stream function at 750 mb. The terrain height h was taken from Berkofsky and Bertoni (1955).

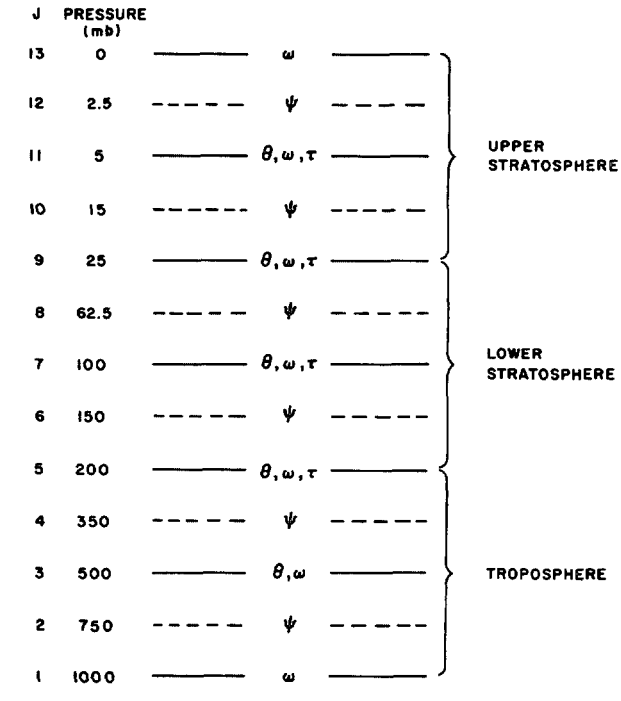

FIGURE 1.—Vertical resolution of the model.

The frictionally induced vertical motion at the top of the Ekman layer, assumed to be 1000 mb, was calculated according to the expression of Charney and Eliassen (1949)

$$\omega_B=-\frac{g\rho_0 \sin 2\alpha}{f}\sqrt{\frac{Kf_0}{2}}\nabla^2\psi_1, \quad (16)$$

where

$f_0=10^{-4}\text{sec}^{-1}$,
K=kinematic eddy-viscosity coefficient (10^5 cm^2 sec^{-1}),
α=cross-isobaric flow angle (22.5°), and
ψ_1=stream function at 1000 mb, taken as $0.5\psi_2$.

Now,

$$\omega_1=\omega_A+\omega_B, \quad (17)$$

where ω_1 is the 1000-mb vertical velocity. Note that equations (15) and (16) must be expressed in spectral form to be used in this model.

Lindzen (1965) showed that visible radiation reflected by the mean observed midwinter cloudiness distribution can produce a temperature disturbance above about 25 km of amplitude 10°K in wave number 2. He suggested that such a disturbance could trigger winter warmings. Thus an added Newtonian heating term, proportional to the difference between the amplitude of the actual temperature harmonic and the harmonic of Lindzen's calculated disturbance, was included in the spectral thermodynamic equation for θ_4^2 at 5 and 25 mb. It tended to produce a wave-number-2 disturbance of maximum amplitude 10°K near 60° N. with warm regions over western Europe and Alaska.

The radiative model of Lindzen and Goody (1965) is only applicable in the upper stratosphere and mesosphere.

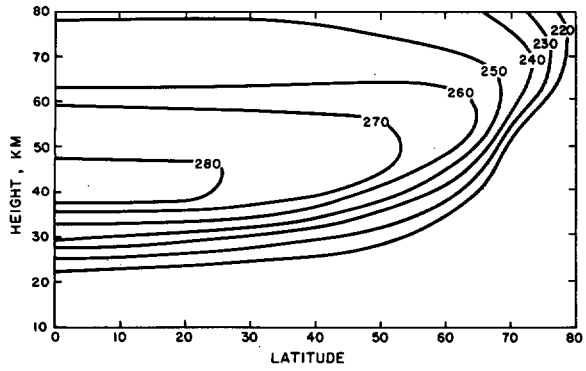

FIGURE 2.—Cross section of radiative-photochemical equilibrium temperature (°K).

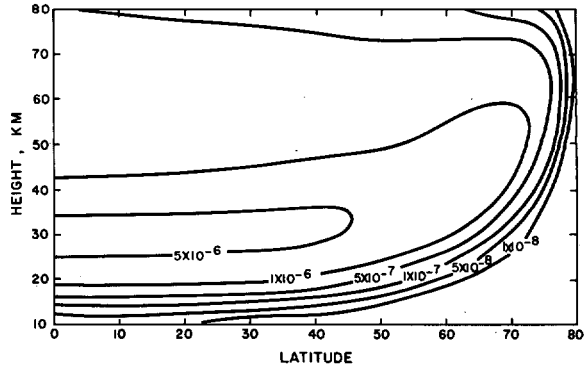

FIGURE 3.—Cross section of radiative-photochemical equilibrium ozone number mixing ratio. Numbers are dimensionless.

At 500 and 200 mb, the total radiative heating was equated to $-h_j(\theta_j-\theta_{ej})$, where θ_{ej} is an equilibrium temperature based on the precise computations of Manabe and Möller (1961). The values of h_j were taken from Peng (1965).

The ozone equation (4) was only considered at levels 5(2)11.[3] A major sink of ozone is near the ground where it is destroyed by chemical processes. In an attempt to incorporate this depletion into the model, the mixing ratio at 500 mb was set at a very low constant value (10^{-8}) for its part in the vertical eddy-diffusive term at 200 mb.

3. RADIATIVE-PHOTOCHEMICAL EQUILIBRIUM

The initial equilibrium solution was accomplished by dividing the region from 10 to 80 km into 23 layers of thickness varying from 10 km at 75 km to 2 km below 45 km. Both the equilibrium ozone amount and temperature τ_e and T_e, respectively, were first found at 75 km, above which it is assumed there is no ozone. The Newton-Raphsen iterative technique (Henrici 1964) was used to find τ_e and T_e at the midpoint of each layer. For the purpose of integrating over frequency to find q_2, q_3, and η, the spectral interval from 1800 Å to 7100Å was divided into 53 subintervals. The data on incident solar flux, ozone, and oxygen cross sections were basically the same as used by Craig (1950), except that for wavelengths $\lambda \leq 2425$Å the data of Brewer and Wilson (1965) were used. After a preliminary run of the experiment, all ozone absorption coefficients were increased by 40 percent, effectively reducing the equatorial equilibrium total ozone from 0.34 to 0.30 cm S.T.P. A more reasonable latitudinal distribution of total ozone in low latitudes was achieved by the model with these data. All the spectral data including the old and new ozone cross sections, α_3 and α_3', respectively, are listed in the appendix. The values of the photochemical constants used were $E=3\times10^{24}$ molecules cm^{-3} and $D=3070$°K from Craig (1950). The radiative constants were $a=1.23\times10^{-6}$ sec^{-1} and $b=2.583\times10^{-4}$ °K sec^{-1}. This value of a is close to the result of Hering et al. (1967) and was assumed independent of height.

[3] The notation 5(2)11 means 5, 7, 9, 11.

The vertical profiles of T_e and τ_e were found at every 5° of latitude from the Equator to the Pole with account being taken of the sphericity of the atmosphere. Diffractive and multiple scattering effects were ignored. Meridional cross sections of the equilibrium results appear in figures 2 and 3.

The equilibrium stream function, ψ_e, was found at the levels $j=4(2)12$ by solving the spectral form of the thermal wind equation (2) after θ_e had been expressed in terms of P_2^0, P_4^0, and P_6^0 at $j=5(2)11$. The stream function at 750 mb, $j=2$, was found by solving the linear balance equation

$$\nabla\cdot(f\nabla\psi)=g\nabla^2Z, \tag{18}$$

where Z, height, was taken from the *U.S. Standard Atmosphere Supplements* (Environmental Science Services Administration et al. 1966) for midwinter conditions. A cross section of the east-west wind for equilibrium conditions appears in figure 4. There is some indication of a weak tropospheric jet near 100 mb and a stratospheric maximum of over 100 m sec^{-1} at 40° latitude associated with the sharp decrease of equilibrium temperature at midlatitudes due to the rapid depletion of the solar radiation by ozone.

The field of vertical motion in the radiative-photochemical equilibrium state was found by solving the ω-equation. It can be thought of as that field necessary to maintain the balance implied by the thermal wind equation as the model is initially integrated from equilibrium. The ω-equation is linear in ω, and thus in its spectral form reduces to five equations, one for each of the east-west wave numbers considered. In symbolic form, they can be written for any number m as

$$A_m\omega_m=B_m,\quad m=0,1,2,3,6. \tag{19}$$

The ω_m is a column matrix containing all 15 if $m=0$ or 10 if $m\neq0$ unknown complex spectral amplitudes of ω at levels $j=3(2)11$. A_m is a 15×15 if $m=0$ or 10×10 if $m\neq0$ matrix calculated once and for all. B_m is a column matrix whose complex elements are functions of radiative heating and the horizontal advection of vorticity and potential temperature. In the initial equilibrium state, only equation (19) with $m=0$ has to be solved since there is no longitu-

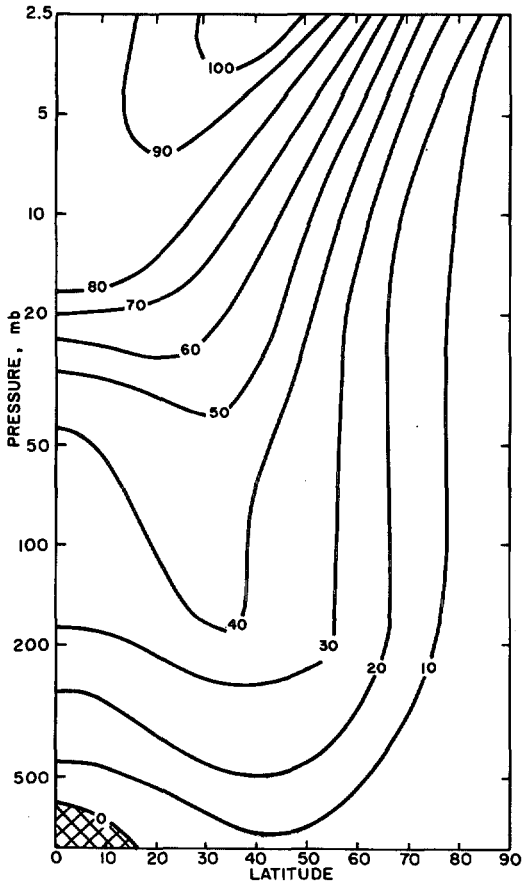

FIGURE 4.—Cross section of east-west wind for radiative-photochemical equilibrium state in m sec^{-1}. Crosshatched areas show easterlies.

dinal dependence. The meridional circulation mainly consisted of a single direct cell.

4. RESULTS

OZONE

Integration of the spectral equations from the initial equilibrium state was accomplished using a fourth-order Runge-Kutta scheme. A favorable aspect of this method is that it yielded very accurate energy integrals over periods of many days, facilitating the construction of energy flow diagrams for the upper and lower stratospheres. The time step was 48 min, and no computational instability difficulties were encountered.

In the manner of Peng (1965), the dynamic eddy-viscosity coefficient, μ, was set inversely proportional to $(\partial\theta/\partial p)_s$ at each level where μ at 750 mb was 225 gm cm^{-1} sec^{-1} from Charney (1959). Table 1 lists the values of μ, $(\partial T/\partial p)_s$, and $(\partial\tau/\partial p)_s$ used at appropriate levels where $(\partial\tau/\partial p)_s$ was taken from Hering and Borden (1964). The ozone eddy-diffusion coefficient was taken as $K_\tau=2\times10^4$ cm^2 sec^{-1} from Prabhakara (1963).

The integration of the model was initiated by introducing a geostrophically balanced perturbation in wave numbers 3 and 6. Heating due to the reflected solar radiation from the cloud tops quickly produced energy in wave number 2 which interacted with the initial

TABLE 1.—*Values of dynamic eddy-viscosity coefficient, μ, and standard lapse rates of ozone number mixing ratio and temperature at appropriate levels*

j	2	4	6	8	10	12
μ, gm cm^{-1} sec^{-1}	225	125	17.5	6.40	0.74	0.156
j	3	5	7	9	11	
$(\partial\tau/\partial p)_s$, mb^{-1}	.....	-1.65×10^{-3}	-2.95×10^{-3}	-1.06×10^{-7}	-4.99×10^{-7}	
$(\partial T/\partial p)_s$, °K mb^{-1}	0.095	0.0033	0	−0.736	−5.5	

perturbation to spread energy throughout the spectrum. For the next 60 days, the zonal and eddy forms of energy underwent substantial adjustments and finally began to oscillate irregularly about quasi-equilibrium values. The initial phase of the experiment then consisted of an additional 120-day run.

Table 2 presents spectral distributions of kinetic and available potential energies at the end of day 150, where A or K represents available or kinetic energy, respectively, and the following subscript denotes either the east-west wave number or the fact that it is zonal energy. The result for this day typifies the last 60 days of the initial phase of the experiment. The available potential energy of any region does not include the contribution from the layer(s) straddling the boundary of that region. The bulk of the tropospheric eddy kinetic energy is in wave number 6, as expected. However, moving up through the stratosphere, the energy shifts toward the longer planetary scale waves. Thus, wave number 6 makes an insignificant contribution to the upper stratospheric total energy. The spectral allotment of available potential energy is similar to that of kinetic energy, except that wave number 1 dominates the troposphere.

The zonally averaged vertical velocities averaged from day 130 to 160 during the quasi-equilibrium period appear in table 3. The stratospheric circulation consists mainly of two cells with generally rising motion from 0° to 20° latitude and from 60° to 90°. The midlatitude subsiding branch is not well defined especially in the lower stratosphere. The tropospheric circulation is mainly a single direct cell. Although on individual days the three-cell circulation that is normally deduced from observations (Kuo 1956) did often occur, the model was not able to maintain this circulation over a long period.

Table 4 gives the distribution of temperature and ozone number mixing ratio on day 180. This result typifies the quasi-equilibrium period. A strong north-south temperature gradient exists at 25 and 5 mb, while the lower stratospheric gradient is weak. The observed midlatitude temperature maximum is not reproduced, probably because of the weakness of the subsiding branch of the meridional circulation in this region.

A cross section of the zonally averaged east-west velocity on day 180 appears in figure 5. On comparison with the equilibrium result in figure 4, it can be seen that there was a northward shift in the stratospheric jet position of from 5° to 10° latitude and a weakening of the maximum wind from 100 to 80 m sec^{-1}. The final jet position, which changed very little during the period from day 120 to 180, compares favorably with the midwinter observations of

Batten (1961). The maximum speed at 2.5 mb is considerably higher than his, however. The jet of Manabe and Hunt (1968) was much weaker than the present one and situated about 15° farther north. A well-defined tropospheric jet has appeared as well as a weak easterly regime in the polar lower stratosphere. These easterlies are transitory and strongly associated with downward-propagating minor stratospheric warmings to be discussed later.

After about day 60, the eddies began to transport ozone from its equatorial source region toward the Pole where the total amount soon achieved typical midwinter values of from 0.40 to 0.45 cm S.T.P. From about day 130 onward, the ozone distribution settled down to a state of quasi-equilibrium. A meridional cross-section of the departure of zonally averaged mixing ratio on day 180 from its initial equilibrium value appears in figure 6. North of 70° latitude, northward transports by the circulation have made up for almost the entire amount of ozone since the equilibrium amount here was almost nil. Ozone is a conservative quantity here as well as throughout most of the lower stratosphere. The largest accumulation at the Pole took place at 100 and 5 mb. In the equatorial region, photochemistry continually attempted to replenish the ozone exported to higher latitudes in proportion to the departure of the mixing ratio from equilibrium; see equation (9). A final balance was struck at amounts only slightly less than in equilibrium; see figure 6.

The latitudinal distribution of total ozone averaged for the last 10 days of the initial experiment is compared in figure 7 with the observations of Godson (1960) and the initial equilibrium solution. The experiment, considering that the initial equilibrium solution is so unlike the observed distribution, has fairly successfully simulated the wintertime total ozone distribution, especially at high latitudes. The spurious secondary maximum at the Equator could either be a fault of the photochemical theory (possibly the theory of Hunt 1966 should be used here) or an outcome of the constraint of symmetry across the Equator. With antisymmetric components present, the eddies possibly would have more freedom to transport equatorial ozone northward. In view of the poor resolution of the model, the vertical distribution of low-latitude ozone agreed well with the mean soundings of Hering and Borden (1964); see figure 8. The high-latitude distribution had a persistent secondary maximum near 15 km, with an overall maximum near 34 km. Individual wintertime high-latitude soundings often show similar secondary maximums, but the overall maximum is usually below 30 km (Hering and Borden 1964). Note the opposite sense of the latitudinal gradient of ozone at 25 and 5 mb in table 4.

A decomposition of the zonally averaged rate of change of ozone averaged from day 130 to 160 at 25 and 200 mb appears in figure 9. These results typify the period when the ozone distribution had settled to a quasi-equilibrium state. At 25 mb, photochemistry is acting as a strong

TABLE 2.—*Energies on day 150 in ergs cm^{-2}*

	Troposphere	Lower stratosphere	Upper stratosphere
A_z	2.97×10^{9}	2.19×10^{7}	3.34×10^{7}
A_1	1.10×10^{8}	2.58×10^{7}	1.11×10^{7}
A_2	5.15×10^{7}	1.96×10^{6}	2.10×10^{6}
A_3	9.34×10^{7}	1.17×10^{8}	2.33×10^{5}
A_6	1.86×10^{7}	4.58×10^{5}	5.28×10^{2}
Total eddy available	2.73×10^{8}	2.93×10^{7}	1.34×10^{7}
K_z	3.19×10^{8}	4.28×10^{8}	2.73×10^{8}
K_1	3.86×10^{6}	5.02×10^{7}	2.70×10^{7}
K_2	9.32×10^{6}	1.96×10^{7}	1.12×10^{7}
K_3	2.98×10^{7}	7.15×10^{7}	1.91×10^{7}
K_6	4.88×10^{7}	9.62×10^{6}	3.30×10^{4}
Total eddy kinetic	9.19×10^{7}	1.51×10^{8}	5.73×10^{7}

TABLE 3.—*Zonally averaged vertical velocities averaged from day 130 to 160 in 10^{-6} mb sec^{-1}*

Latitude	0	10	20	30	40	50	60	70	80	90
5 mb	− 0.12	− 0.07	0.03	0.10	0.09	0.02	−0.06	−0.08	− 0.07	− 0.05
25 mb	− 1.29	− 0.64	0.65	1.28	0.63	−0.63	−1.18	−0.39	1.04	1.75
100 mb	4.86	3.00	− 0.93	− 3.59	− 3.00	−0.27	1.71	1.18	− 0.88	− 1.99
200 mb	− 6.36	− 4.37	0.14	3.99	4.82	2.72	−0.31	−2.37	− 3.06	− 3.12
500 mb	−42.45	−29.26	− 1.12	18.85	18.06	5.90	3.10	20.01	45.46	57.58
1000 mb	36.35	18.62	−16.70	−34.10	−16.50	17.07	30.30	6.23	−34.95	−55.00

TABLE 4.—*Distribution of temperature (T) in °K and ozone number mixing ratio × 10^{6} (τ) on day 180. Total ozone (cm S.T.P.) above 250 mb is also shown*

Latitude		0	10	20	30	40	50	60	70	80	90
5 mb	T	263.4	263.0	216.5	258.1	252.2	243.5	232.9	222.4	214.6	211.7
	τ	1.45	2.09	3.50	4.60	4.72	4.17	3.79	4.11	4.84	5.21
25 mb	T	228.3	227.1	224.4	221.3	218.9	217.2	215.7	213.9	212.2	211.5
	τ	5.33	5.14	4.60	3.86	3.10	2.46	2.06	1.87	1.82	1.82
100 mb	T	211.6	211.5	211.3	211.5	212.4	213.9	215.4	216.6	217.2	217.4
	τ	0.93	0.85	0.74	0.86	1.36	2.14	2.92	3.47	3.73	3.80
200 mb	T	221.7	221.6	220.2	215.9	209.0	202.4	199.6	201.8	206.0	208.1
	τ	0.12	0.11	0.09	0.09	0.15	0.22	0.26	0.25	0.22	0.20
500 mb	T	267.8	267.7	267.0	264.5	259.5	252.1	243.5	235.3	229.5	227.4
Total ozone		0.288	0.281	0.265	0.257	0.268	0.299	0.337	0.370	0.391	0.398

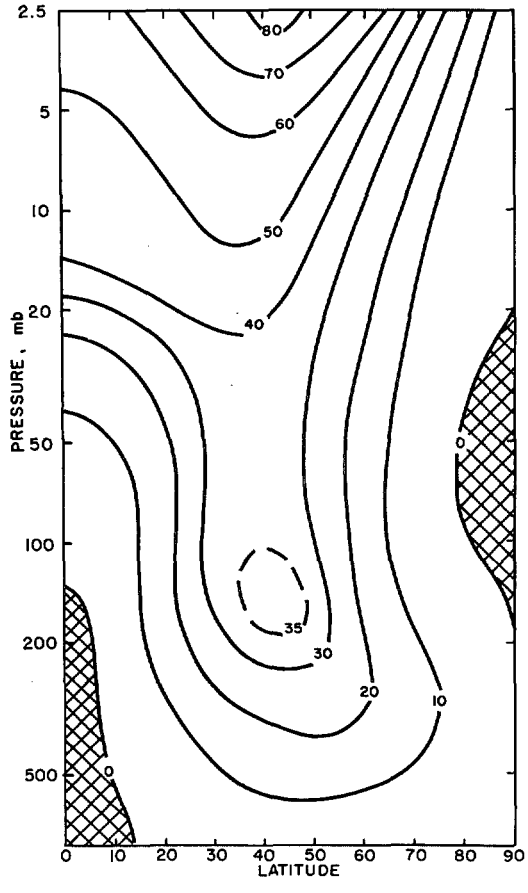

FIGURE 5.—Cross section of zonally averaged east-west wind on day 180 in m sec^{-1}. Crosshatched areas show easterlies.

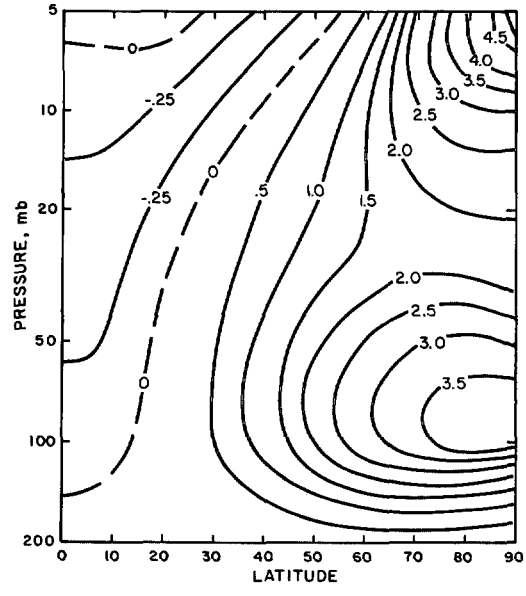

FIGURE 6.—Departure of ozone number mixing ratio times 10^6 on day 180 from radiative-photochemical equilibrium solution. Numbers are dimensionless.

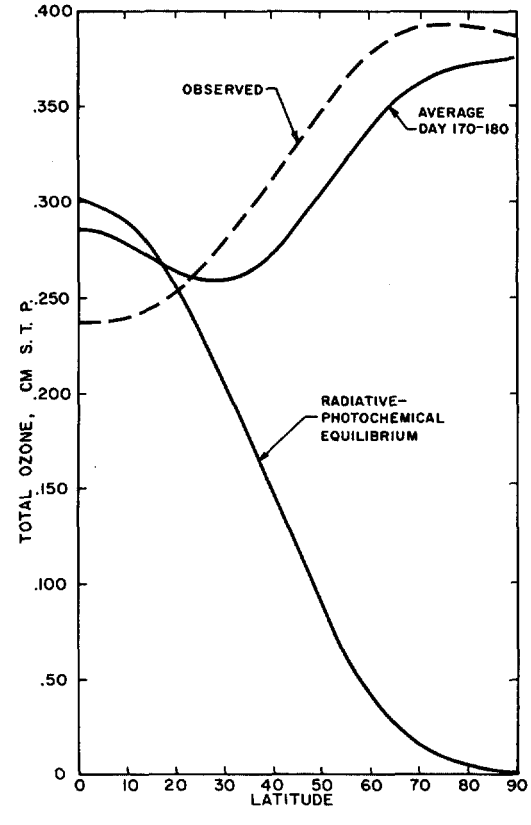

FIGURE 7.—Comparison of latitudinal distribution of total ozone averaged from day 170 to 180 with equilibrium distribution and observed midwinter distribution from Godson (1960).

source of ozone south of 30° N. and as a sink elsewhere. North of 70° latitude, where the incoming solar radiation is zero for the solar declination used, the photochemical terms in equation (9) should be zero. However, the truncated series of zonal harmonics cannot represent a fall of B and C (and η) to zero near 70°, and a spurious photochemical depletion of ozone occurs near the Pole at 25 mb. The planetary scale eddies at 25 mb are actively transporting most of the photochemically produced equatorial ozone out of the Tropics to midlatitudes. Small-scale vertical diffusion is also helping to counter the equatorial ozone source. At the same time, the horizontal eddies are exporting ozone out of the polar region to give a net accumulation at midlatitudes over the 30-day period. In contrast to the results of Hunt (1969), transports of ozone by the mainly two-cell stratospheric meridional circulation play a secondary role in the 25-mb budget. Remember that horizontal transports by the mean meridional circulation are neglected in this model.

In view of the long-term accumulation at midlatitudes, how does the stratosphere transport ozone from its equatorial source region, near 25 mb, to the polar lower stratosphere to maintain the polar maximum in total ozone during the quasi-equilibrium period? This process takes place in two steps. First, the accumulation of ozone at midlatitudes in figure 9 does not persist indefinitely. Occasional spontaneous high-latitude warmings occur every 10 to 20 days. These are associated with an intensification of the eddies and an almost complete reversal of their horizontal advectional pattern. Figure 10 decomposes the 25-mb rate of change of ozone at the peak of one such warming. This intense warming took place on day 125. Similar less-intense ones occurred during the averaging period. Now the eddies are very rapidly de-

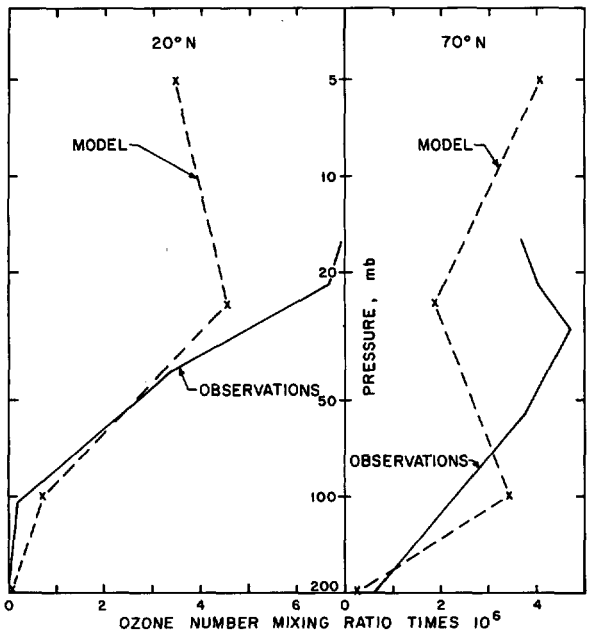

FIGURE 8.—Comparison of vertical distributions of ozone number mixing ratio at 20° and 70° N. with mean observations of Hering and Borden (1964). Numbers are dimensionless.

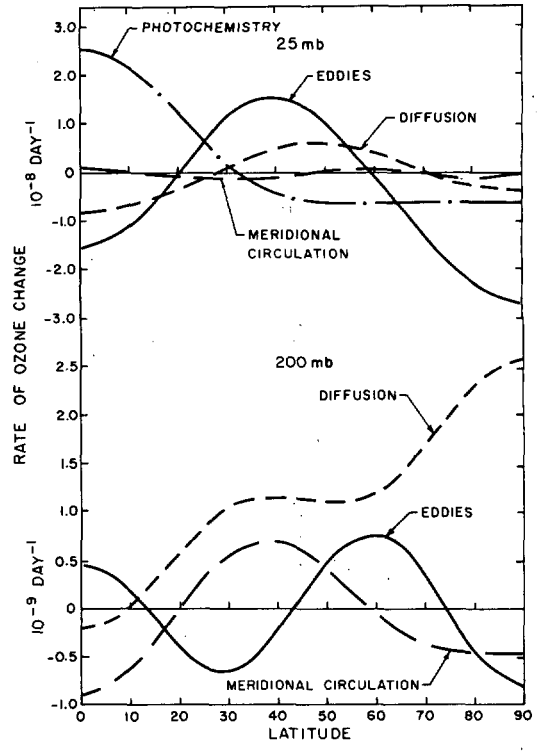

FIGURE 9.—Decomposition of the zonally averaged rate of ozone change at 25 and 200 mb averaged from day 130 to 160.

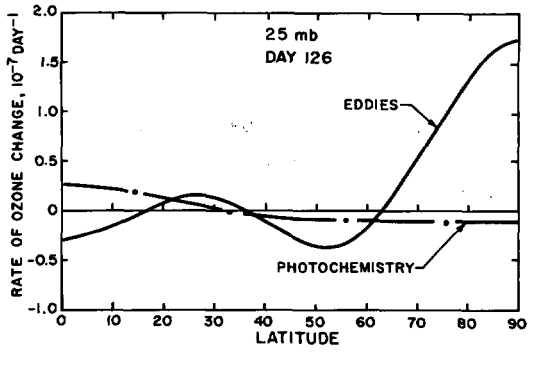

FIGURE 10.—Decomposition of the zonally averaged rate of ozone change at 25 mb, day 126.

pleting the midlatitude store of ozone and accumulating it at the Pole.

The second step in the transport of ozone to the polar lower stratosphere is shown in the 200-mb budget averaged from day 130 to 160 in figure 9. The large amounts of ozone deposited during the warmings at the Pole at 25 mb are being gradually diffused downward into the polar lower stratosphere, where advective effects of the eddies and two-cell meridional circulation are small and photochemical effects are inoperative.

Thus in this experiment, the transport of ozone from its equatorial source region to the polar lower stratosphere during the quasi-equilibrium period is achieved by the horizontal planetary scale eddies and by small-scale vertical eddy-diffusive effects, much in the manner envisaged by Newell (1963). Vertical transports by the two-cell meridional circulation with rising motion near the Pole and Equator and sinking at midlatitudes were of secondary importance in the ozone budget. Occasional high-latitude warmings to be discussed in detail later played a vital role in the ozone budget.

MEAN ENERGY CYCLES

Energy cycles for the upper and lower stratosphere appear in figures 12 and 13 averaged from day 130 to 160. Each diagram conforms to the model of figure 11, where the meaning of most of the symbols is explained below and energy transfers are considered positive in the direction of the arrow. The various symbols are:

A_z or A_n zonal available potential or eddy available potential energy in wave number n, respectively,

K_z or K_n zonal kinetic or eddy kinetic energy in wave number n, respectively,

R radiative generation,

F generation through nonlinear interactions,

D eddy-viscous generation, and

B boundary generation due to upward fluxes of kinetic energy and conversions from available to kinetic energy in the layer straddling the boundary.

A complete derivation and discussion of the energy equations in the spectral domain is found in Clark (1969).

Wave number 6 has been omitted from the upper stratosphere energy cycle in figure 12 because of its insignificant role. Even though these are long-term mean cycles, the net rate of change of any energy component (not shown) is not necessarily very small. Shown in each box is the mean value of that energy component for the period.

Lindzen and Goody (1965) showed that the coupling of radiative and photochemical effects should lead to an enhanced Newtonian dissipation of upper stratospheric

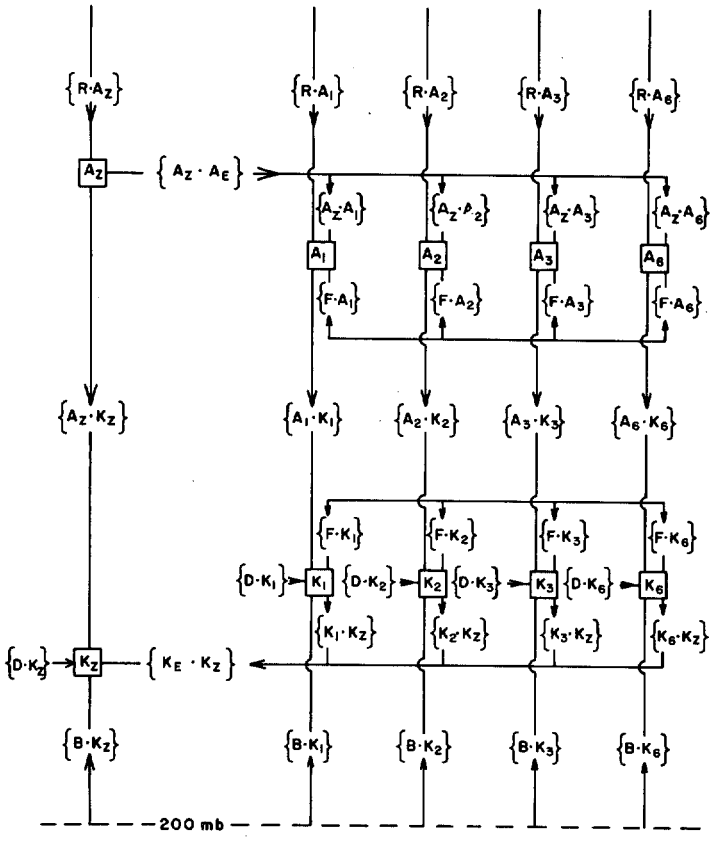

FIGURE 11.—Energy cycle model in the spectral domain. All symbols are explained in the text.

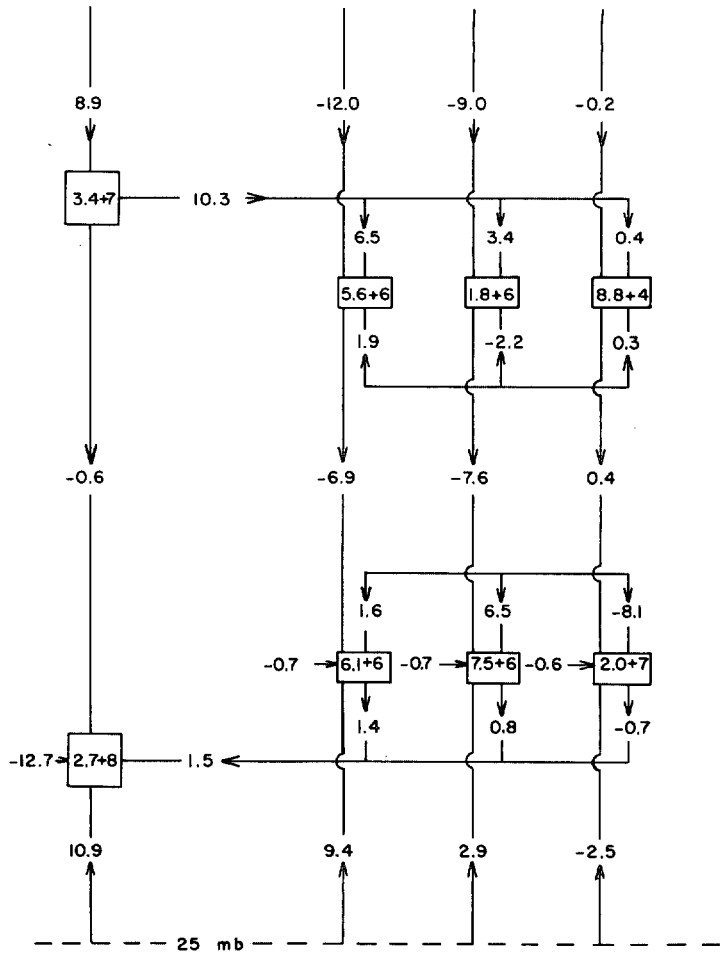

FIGURE 12.—Mean upper stratospheric energy cycle. See figure 11 for the model. Units, transformations —ergs cm^{-2} sec^{-1}, energies —ergs cm^{-2}. Numbers $x+n$ mean x times 10^n.

temperature disturbances. This can be visualized in the following manner: relatively warm (cold) regions at any pressure level will tend to have low (high) ozone concentrations through the temperature dependence of photochemistry in equation (9), and thus these regions will cool (warm) relative to the surroundings because of the solar heating term in equation (8). Because of the smaller insolation at lower levels or higher latitudes, this coupling will hardly be as effective as in the equatorial upper stratosphere, and temperature anomalies will be mainly controlled by atmospheric motions. The strong radiative dissipation of eddy available energy in figure 12 is in part due to this coupling of radiative and photochemical effects. In wave numbers 1 and 2, this dissipation is opposing any tendency to create eddy kinetic energy baroclinically through direct east-west overturnings. In fact, indirect overturnings are being induced in these waves that are countering the diabatic eddy available energy sink. Only wave number 3 is transforming zonal-available to eddy kinetic energy in the baroclinic sense in the upper stratosphere. However, the effect of wave numbers 1 and 2 dominates. Thus, in the mean, the winter upper stratosphere is an energy sink and has to be maintained by interactions with the lower stratosphere.

The upper stratospheric zonal kinetic energy is being maintained against eddy-viscous dissipation of 12.7 ergs cm^{-2} sec^{-1} mainly by an upward flux of zonal kinetic energy across 25 mb and to a lesser extent by the forced barotropic conversion of eddy to zonal kinetic energy in wave numbers 1 and 2. Thus the polar vortex, in the mean, is barotropically stable. Note that in a quasi-geostrophic model the pressure-interaction term which can transfer significant amounts of energy between regions (Manabe and Hunt 1968) is neglected.

Wave number 3 in the upper stratosphere participates in an entirely different energy cycle than numbers 1 and 2. It is baroclinically and barotropically creating eddy kinetic energy and serves as a significant source of kinetic energy for waves 1 and 2 through nonlinear interactions. It also exports energy to the lower stratosphere.

The most notable feature of the mean lower stratospheric energy cycle in figure 13 is the strong forcing of the region from below needed to counter both the eddy-viscous dissipation of zonal kinetic energy and, to a lesser extent, the export of kinetic energy to the upper stratosphere. Radiative effects are of secondary importance to the energetics and, as observed by Oort (1964), are a source of eddy available and a sink of zonal available energy. The diabatic generation of eddy available energy arises because of a positive correlation between temperature and ozone at 100 mb (photochemistry is unimportant at this level) and the resulting solar heating (cooling) of warm (cold) areas. The reversed latitudinal temperature

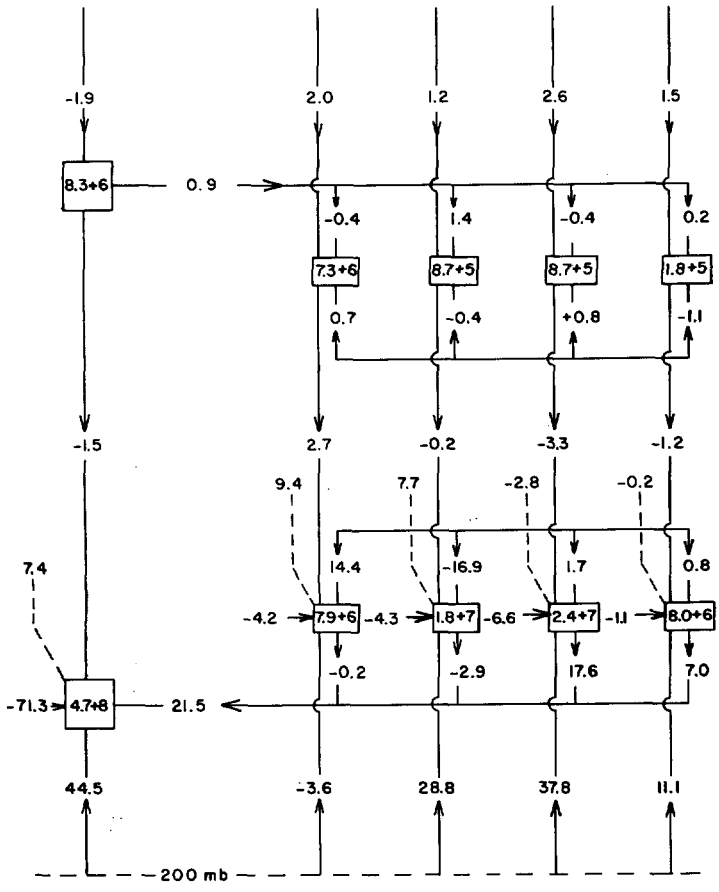

FIGURE 13.—Mean lower stratosphere energy cycle. See figure 11 for the model. Dashed lines show exports of kinetic energy across 25 mb. Units, transformations —ergs cm^{-2}. Numbers $x+n$ mean x times 10^n.

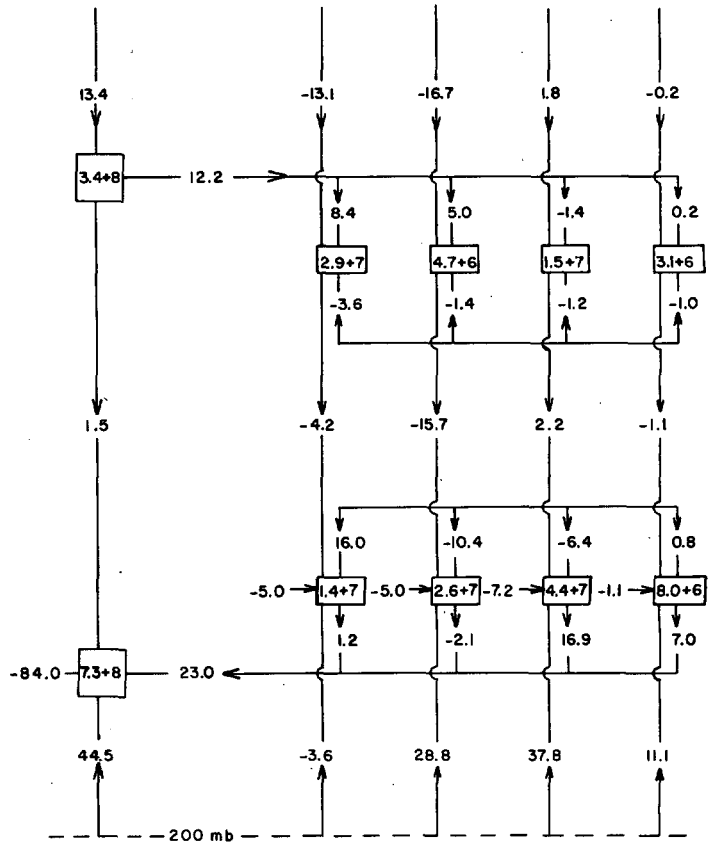

FIGURE 14.—Mean energy cycle of the entire stratosphere. See figure 11 for the model. Units, transformations —ergs cm^{-2} sec^{-1}, energies —ergs cm^{-2}. Numbers $x+n$ mean x times 10^n.

gradient leads to a radiative dissipation of zonal available energy.

As observed by Reed et al. (1963) and Oort (1964), the winter lower stratosphere does not have an internal source of kinetic energy and, as in the upper stratosphere, the strong eddy-viscous dissipation of zonal kinetic energy, 71.3 ergs cm^{-2} sec^{-1}, is countered by an upward flux of kinetic energy from the troposphere and the barotropic conversion of eddy to zonal kinetic energy. This conversion is carried out by wave numbers 3 and 6, whereas in the upper stratosphere, wave numbers 1 and 2 were accomplishing the transformation.

Not withstanding the fact that the lower stratosphere is more massive than the upper stratosphere, the mean energy cycle of the entire stratosphere in figure 14 has many features of the upper stratospheric cycle. Since regular balloon observations rarely get above 10 mb, observed stratospheric energy cycles usually include the lower stratosphere only.

Intense radiative dissipation of eddy available energy at 25 mb as well as at 5 mb has overcome the slight generation at 100 mb to give a net depletion in figure 14. Similarly, there is a net radiative generation of zonal available energy for the entire stratosphere. Whereas the meridional circulation at 5 and 100 mb is indirect, a strong direct circulation at 25 mb gives a net creation of zonal kinetic at the expense of zonal available energy. Nonlinear interactions between the various wave components serve to transfer kinetic energy from wave numbers 2 and 3, which are being strongly driven from below, up the scale to drive wave number 1. As for the lower stratosphere alone, wave numbers 3 and 6 are being forced by the troposphere to advect momentum against the gradient to help maintain the stratospheric jet against eddy-viscous dissipation.

Significant conclusions to be drawn from this study of the mean stratospheric energy cycle are:

1) The joint radiative-photochemical dissipation of upper stratospheric temperature disturbances strongly inhibits the baroclinic development of kinetic energy and results in the region being driven by the lower stratosphere.

2) The entire winter stratosphere is mainly driven by the troposphere.

3) The zonal kinetic energy of the winter stratosphere is maintained against eddy-viscous dissipation by an upward flux of zonal kinetic energy and by the forced barotropic conversion of eddy energy, mainly by wave numbers 3 and 6.

4) Nonlinear interactions with wave numbers 2 and 3 are the main source of kinetic energy for wave number 1.

STRATOSPHERIC WARMINGS

Spontaneous high-latitude warmings—After the 120th day of the experiment, occasional spontaneous minor warmings occurred near the Pole. They usually originated at the highest level (5 mb) and propagated downward

reaching 100 and 200 mb from 4 to 7 days later. Figure 15 illustrates, in terms of isolines of the departure of the polar temperature from equilibrium, one that began on day 143. The temperature wave attained its highest amplitude, 12°K, at 25 mb. Hardly any response was noted at 200 mb, and the troposphere was largely unaffected.

Other manifestations of the warming were:

1) A temporary increase in total ozone at the Pole from 0.371 to 0.416 cm S.T.P. This effect was discussed in connection with the mean ozone budget.

2) A temporary weakening of the jet maximum at 5 mb from 84 m sec^{-1} to 75 m sec^{-1}.

3) A temporary strengthening of the weak easterly flow near the Pole in the lower stratosphere.

During the period of rapid temperature rises associated with this warming, the two-cell mean meridional circulation in the stratosphere reversed to give subsidence in the equatorial and polar regions. Mahlman (1969) noted that an area of subsidence temporarily appeared near the Pole in the lower stratosphere during a minor warming in 1958. The polar warming at 5 mb was the result of an excess of adiabatic compressional heating due to subsidence (12° per day) over cooling due to the eddy advection of heat away from the Pole (10° per day). Figure 16 decomposes the heating at 5 mb at the peak of this warming. The subsequent decline of polar temperatures was associated with a reversion back to the normal meridional circulation and related adiabatic cooling due to the rising air at the Pole. Again, eddy advections of heat partially compensated for the adiabatic cooling. As can be seen in figure 16, radiative heating played a minor role in the warming. Primarily the same mechanism caused the warming at 25 mb; whereas at 100 mb, the slight temperature wave at the Pole resulted from the eddy advection of heat from midlatitudes.

This conclusion about the nature of the rapid temperature rises near the Pole agrees, in part, with the finding of Craig (1965). He suggested that areas of rapid temperature rises at 25 mb connected with the 1957 warming could plausibly be associated with adiabatic compressional heating.

A better understanding of the warming is to be gained by examining the energy cycles. Prior to each spontaneous warming, a notable feature was the large increase in upward flux of eddy kinetic energy across 200 mb. This was particularly noticeable in wave numbers 2 and 3 that alternately underwent order of magnitude increases. The energy cycle of the upper stratosphere on day 143, when the most rapid temperature rises were noted at the Pole, appears in figure 17. The boxes now show the rate of change of energy in each component. Note the sizeable upward flux across 25 mb of kinetic energy in wave number 3 compared to the small downward flux in the mean cycle of figure 12. Somehow, the increased forcing has promoted a strong nonlinear interaction between wave numbers 1, 2, and 3 that is transferring a large amount of kinetic energy, 92.9 ergs cm^{-2} sec^{-1}, to wave number 1 while depleting the energy in waves 2 and 3 regardless of the increased forcing of these waves.

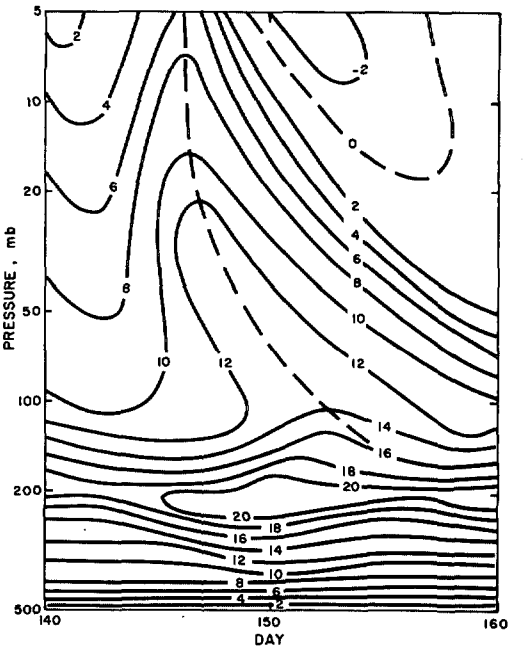

FIGURE 15.—Departure of polar temperature from equilibrium (°K) during spontaneous warming.

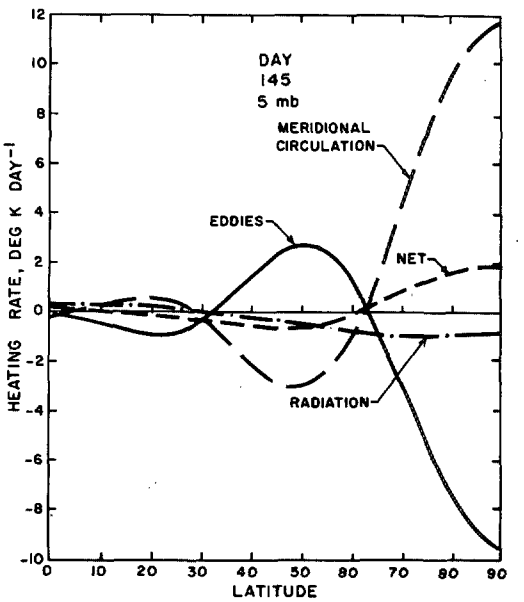

FIGURE 16.—Decomposition of the zonally averaged heating rate, day 145 at 5 mb.

Part of this flood of energy into wave number 1 is being exported to the lower stratosphere, more than compensating for the upward fluxes in the other components. The upper stratosphere has temporarily become a source of kinetic energy.

A large portion of the energy gained in wave number 1, 41.8 ergs cm^{-2} sec^{-1}, is being transferred to eddy available energy, and part of this is driving wave number 1 to advect heat away from the Pole to give a net creation of zonal available energy at the rate of 3.8 ergs cm^{-2} sec^{-1}. At the same time, the upper stratospheric zonal kinetic energy is being transformed barotropically into eddy kinetic energy,

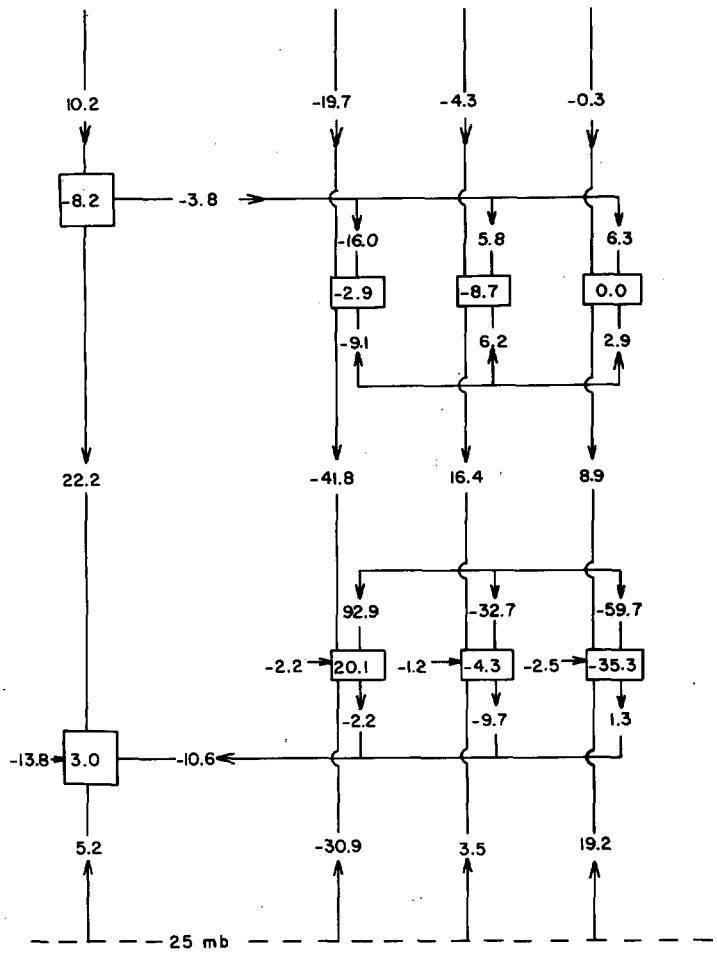

FIGURE 17.—Energy cycle of the upper stratosphere on day 143. See figure 11 for the model where boxes now show the rate of change of the energy component. Units, $-$ergs cm^{-2} sec^{-1}.

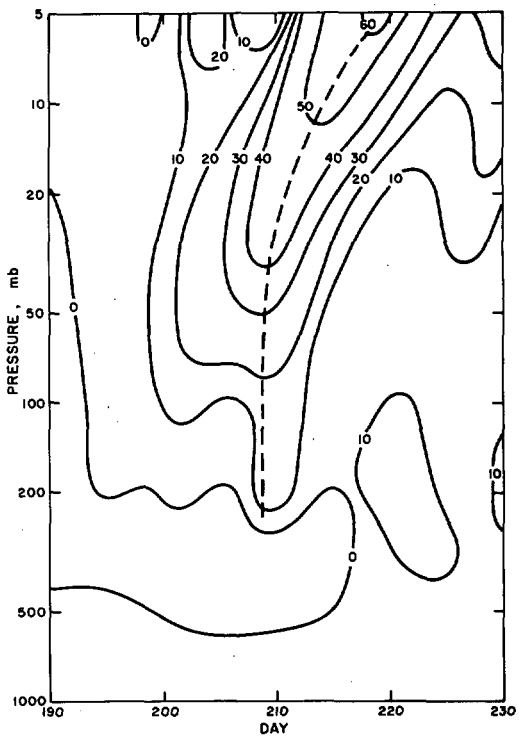

FIGURE 18.—Departure of polar temperature from equilibrium on day 180 (°K) during stratospheric warming.

and a direct meridional circulation is driven that more than compensates for the eddy cooling near the Pole to give a net heating.

The reaction of the lower stratosphere to the increased tropospheric forcing, although similar in some respects to that of the upper stratosphere, was delayed by a few days. It seems that the response of the lower stratosphere was dependent upon the existence of a downward flux of energy across 25 mb. A similar, rapid nonlinear growth of wave number 1 took place, but the response of the mean meridional circulation to the increased eddy momentum and heat fluxes was not as strong.

In summary, the following conclusions can be drawn concerning the nature of the spontaneous warmings:

1) They were not entirely local in origin and were related to increased forcing of the stratosphere by the troposphere.

2) They propagated downward with a phase speed of about 3 km per day.

3) Rapid nonlinear exchanges of kinetic energy between the planetary scale waves were vital to the development of a warming.

4) The rapid temperature rises near the Pole were associated with adiabatic compressional heating in the mean meridional circulation.

A FULL-SCALE STRATOSPHERIC WARMING

At no time did a spontaneous high-latitude warming develop into a full-scale stratospheric warming so that, for instance, the latitudinal temperature gradient reversed and the polar vortex was replaced by an easterly regime. Following the suggestion by Charney and Stern (1962) that the stability of an internal jet was strongly influenced by the temperature gradient near the ground, polar equilibrium conditions were altered on day 180 to simulate a cooling by 20°K through a deep layer extending from the ground to 500 mb. The zonally averaged stream function field was then adjusted to maintain the geostrophic balance between the wind and thermal fields at all levels. The result was an increase in the maximum jet speed at 2.5 mb by 30 m sec^{-1} and a strengthening of the north-south wind shear at all latitudes. The experiment was then run for an additional 50 days to day 230.

After day 200, rapid temperature rises of 10° to 20°K occurred in the lower stratosphere near the Pole, with highest temperatures attained on day 209; see figure 18. This warming rapidly intensified as it spread upward to the upper stratosphere and precipitated polar warmings of 40° and 60°K at 25 and 5 mb, respectively. Maximum temperatures at 5 mb were attained on day 219 about 10 days later than at 200 mb. The most rapid heating occurred at 5 mb at a rate of about 50°K in 5 days, in agreement with observed peak heating rates during actual sudden warmings, London and Prabhakara (1964). The latitudinal temperature gradient at 25 mb was completely but only temporarily reversed, while at 5 mb it changed sign north of 50° latitude only.

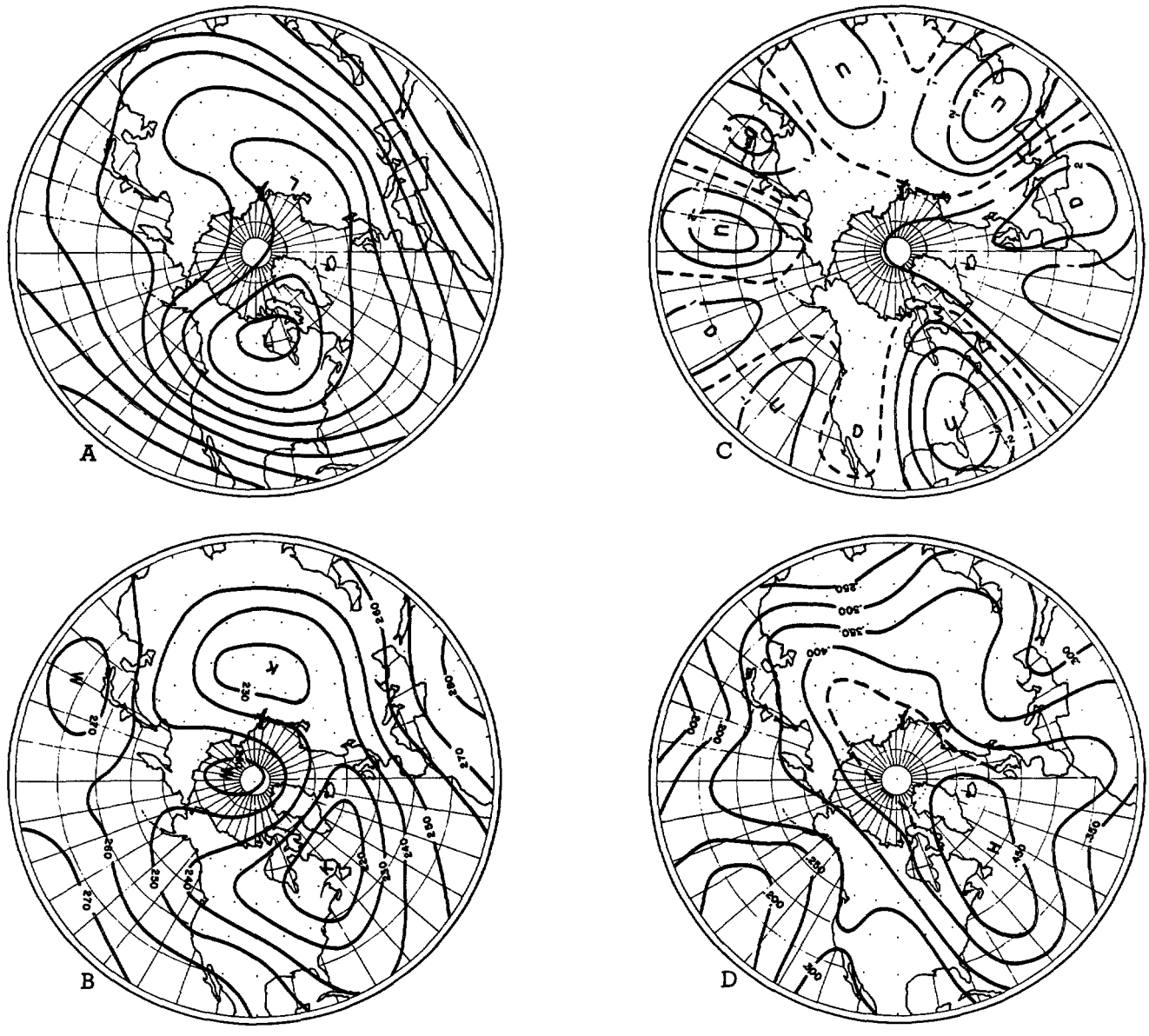

FIGURE 19.—Maps of (A) stream function 2.5 mb, day 220, with contour interval 5×10^{11} cm^2 sec^{-1}; (B) temperature 5 mb, day 220, in °K; (C) vertical velocity 5 mb, day 220, in 10^{-5} mb sec^{-1}; and (D) total ozone, day 220, in cm S.T.P.

The synoptic situation on day 220 is summarized in figure. 19. Prior to the warming, the stratospheric flow pattern consisted of strong westerlies encircling an eccentric polar vortex. As the warming proceeded from day 210 to 220, the vortex elongated into a principally wavenumber-2 pattern and split into two centers over Asia and North America (fig. 19A). At the same time, the warm Alaskan ridge extended northward to the Pole, isolating cold pools over Asia and North America and leaving a warm pocket near the Pole in figure 19B. Pronounced cells of rising motion associated with the cold Lows over Asia and North America dominate the vertical motion pattern at 5 mb on day 220 in figure 19C. Vertical motions in the lower stratosphere were out of phase with those in the upper stratosphere, giving strong subsidence in each Low.

The warming resulted in an augmented accumulation of ozone near the Pole at all levels, mainly as a result of increased horizontal eddy advection from midlatitudes. The polar amount attained its maximum value of 0.47 cm S.T.P. on day 209. The hemispheric distribution of total ozone in figure 19D shows an area near 50° latitude with amounts greater than 0.45 cm S.T.P. associated with the nearby cold stratospheric Low over North America. Widespread lower stratospheric subsidence over this region is advecting ozone-rich air from the higher levels and, at the same time, producing relatively high lower stratospheric temperatures through compressional heating. In the 1958 warming, London and Prabhakara (1964) noted a similar relation between high ozone amounts and high 25-mb temperatures and attributed the correlation to large-scale vertical motions. Note, however, that a cool pool overlies this region in the upper stratosphere in figure 19B.

The stratospheric jet was weakened considerably by the warming and temporarily shifted southward. It did not, however, break down completely to be replaced by a summer easterly regime and regained some of its original

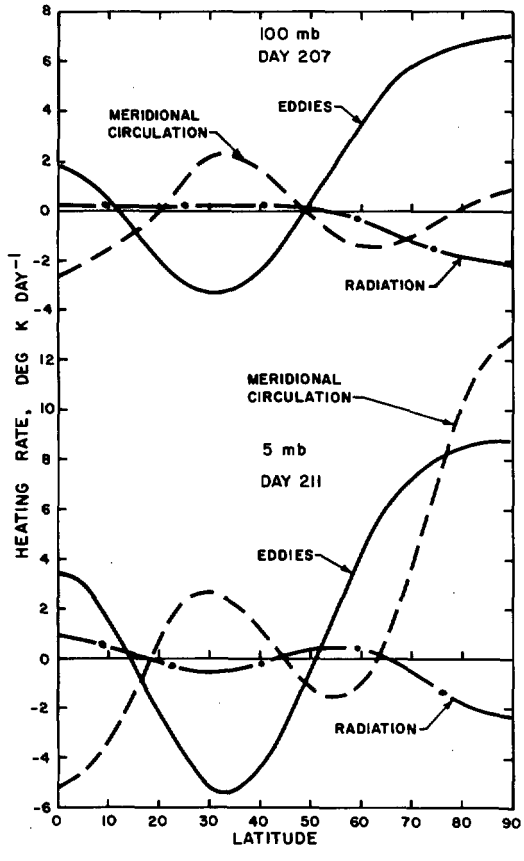

FIGURE 20.—Decomposition of the zonally averaged heating rate at selected levels during the stratospheric warming.

TABLE 5.—*Major energy cycle components during warming, ergs cm^{-2} sec^{-1}*

Day	$\{A_Z \cdot A_E\}$	$\{A_E \cdot K_E\}$	$\{A_Z \cdot K_Z\}$	$\{B \cdot K_E\}$	$\{K_E \cdot K_Z\}$	$\{B \cdot K_Z\}$
			Upper stratosphere			
201	44.7	−159.4	43.2	183.1	− 50.0	183.2
203	168.2	−193.1	− 68.6	386.9	− 12.6	− 220.2
205	54.5	142.4	−105.5	194.5	76.6	13.4
207	− 30.4	14.8	− 75.1	206.6	559.2	67.7
209	90.7	− 11.6	−125.0	68.8	234.5	120.2
211	42.4	20.5	74.9	5.9	− 66.9	− 8.4
213	77.3	−158.4	− 11.3	136.5	−111.9	96.2
215	−129.6	−105.9	91.0	182.1	−211.4	− 70.9
217	33.7	− 47.7	− 70.5	− 74.0	76.0	− 8.8
219	8.3	− 84.4	− 24.0	− 60.0	−153.8	− 107.1
221	− 11.5	− 54.9	− 7.4	39.4	−101.7	− 134.5
			Lower stratosphere			
201	10.6	179.1	−183.4	1509	740.7	− 170.3
203	154.4	12.5	9.2	− 1837	− 72.1	578.4
205	− 13.2	−133.5	− 2.3	543	− 55.7	− 176.5
207	−353.5	−187.5	48.0	3641	1077.0	− 129.6
209	− 54.8	77.6	60.2	957	−834.7	451.2
211	148.3	310.7	− 35.9	− 2260	−449.2	1283.0
213	120.1	− 19.7	− 74.8	− 1517	−654.8	1124.0
215	−137.5	− 55.1	81.0	2289	628.1	−1190.0
217	−254.1	−121.3	104.1	3243	655.8	−1524.0
219	−246.1	−213.1	13.1	253	−130.4	63.0
221	50.1	− 96.8	− 60.5	− 954	−176.2	560.0

strength toward the end of the experiment. A weak easterly flow of about 10 m sec^{-1} appeared for a short period near the Pole in the upper stratosphere.

The typical two-cell mean meridional circulation persisted through most of the warming except during the period of maximum temperature rises when it reversed to give strong subsidence at the Pole in the same manner as in the spontaneous high-latitude warmings.

Although this simulated warming propagated upward, actual sudden warmings have been observed to spread both upward and downward. Craig and Lateef (1962) established that the temperature rises associated with the 1957 warming originated at the highest observed levels, whereas Hirota (1967*b*) found that the 1963 warming propagated upward. It is tempting to attribute the opposite course of these warmings to different driving mechanisms; however, their directions are more likely a reflection of the stability of the upper and lower stratosphere prior to the onset of the warming.

Unlike most observed major warmings in which the rapid temperature rises originate between 50° and 60° latitude and slowly engulf the Pole a week or so later (Finger and Teweles 1964), this warming occurred very close to the Pole. Only strong cooling was noted at midlatitudes in association with the splitting off of the two vortices.

The zonally averaged heating rate at 100 and 5 mb during the period of most rapid temperature rises at each level, is decomposed in figure 20. The warming at 100 mb is being accomplished by a rapid influx of heat from midlatitudes by the horizontal eddies in the same manner as with spontaneous warming. At first, since the Pole is relatively cold at 100 mb, the eddies are destroying A_Z, but they continue advecting northward after the latitudinal temperature gradient has reversed and thus create A_Z. Table 5 lists the major components of the lower and upper stratosphere energy cycles during the warming and shows that the conversion $\{A_Z \cdot A_E\}$ changed sign from day 201 to 207. Strong subsidence heating at the 5-mb Pole combined with equally intense northward horizontal eddy advection of heat together give a peak net heating of 19.5° per day on day 211 in figure 20. This is a major departure from the behavior of the spontaneous high-latitude warmings when the eddies exported heat away from the polar cap almost as fast as adiabatic compressional heating could create it. Now in table 5, the eddies on day 211 as well as the meridional circulation are destroying A_Z in the upper stratosphere. One purpose of this presentation is to attempt an explanation of this departure from the usual behavior and thus account for the exceptional intensity of the warming.

As table 5 shows, the energy cycles of the lower and upper stratospheres are quite variable throughout the whole warming period. The cycles before and after the warming do not have any overall distinguishing features. Lower boundary effects, especially at 200 mb, are about two to three orders of magnitude larger than in the average winter cycle; and throughout the warming period, the cycles of both regions responded quite closely to fluctuations in the forcing from below. The increased tropospheric latitudinal temperature gradient has favored the rapid baroclinic development of tropospheric eddy kinetic energy, part of which is occasionally leaking up into the stratosphere.

The energy cycle of the lower stratosphere on day 207, at the peak of the warming in this region, appears in figure 21. On this day, the upward flux of eddy kinetic energy across 200 mb reached the maximum of the entire warming period. This flux is greatest in wave number 3 and is forcing a strong indirect east-west overturning in this wave, which is creating eddy available energy at the rate of 134.3 ergs cm^{-2} sec^{-1}. Infrared cooling is not dissipating the additional available energy in wave number 3 rapidly enough to prevent the eddies from being compelled to advect heat into the lower stratospheric polar region and create A_Z at the rate of 204.1 ergs cm^{-2} sec^{-1}. The increased upward flux of K_E across 200 mb is also forcing a strong barotropic creation of K_Z by the eddies. However, a large flux of K_Z down into the troposphere more than compensates for the additional K_Z, and a direct mean meridional circulation is forced that partially compensates for the additional eddy heating at the Pole. Thus, the warming in its initial stage in the lower stratosphere is forced by the troposphere.

Part of the enhanced upward flux of K_E across 200 mb leaked into the upper stratosphere from day 207 to 209. The response of this region to the additional forcing was quite different. Initially, the additional energy was stored in the form of K_Z by forced eddy momentum fluxes. See the large positive values of $\{K_E \cdot K_Z\}$ in table 3. Unlike the lower stratosphere, the additional K_Z was not transferred back across 25 mb. Between day 209 and 211, the upper stratospheric eddies suddenly began to destroy K_Z barotropically; and for the next 10 days, the conversion $\{K_E \cdot K_Z\}$ was strongly negative (table 5). On day 211 (fig. 22), the barotropic sink of K_Z is being balanced by a forced direct meridional circulation that by heating the Pole 13° per day is transforming A_Z into K_Z at the rate of 74.9 ergs cm^{-2} sec^{-1} in the opposite sense of the normal circulation. At the same time, the upper stratosphere is baroclinically destroying A_Z, that is, $\{A_Z \cdot A_E\}=42.4$ ergs cm^{-2} sec^{-1}, and the eddies are also heating the Pole 8.8° per day (fig. 20). The barotropic destruction of the polar-night jet continued at an increased rate for the next 10 days; however, the sense of the mean meridional circulation reversed to give adiabatic cooling at the Pole, offsetting the continued eddy heating. Thus, the exceptional intensity of the upper stratospheric warming can be attributed in part to the polar-night jet suddenly becoming barotropically unstable. A buildup of the intensity of the jet due to the leakage of kinetic energy from the lower stratosphere probably caused the lateral wind shear to become supercritical in some sense and the warming proceeded by internal conversions of energy.

The following conclusions follow from this simulated stratospheric warming:

1) At least in its initial stage in the lower stratosphere, the warming is mainly driven from the troposphere.

2) An outbreak of barotropic instability, in the sense that $\{K_E \cdot K_Z\}$ became negative in the upper stratosphere,

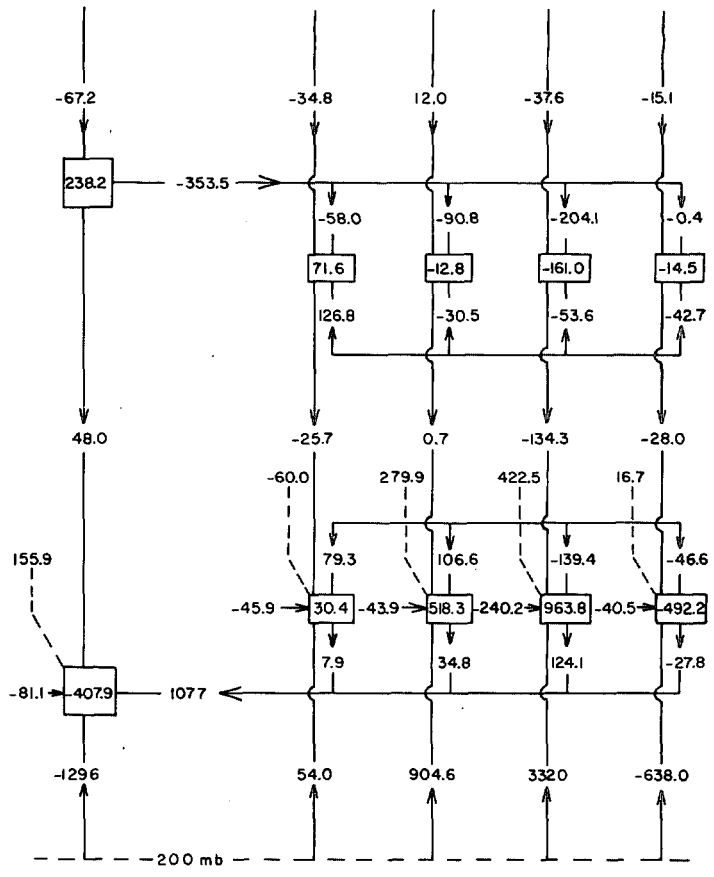

FIGURE 21.—Energy cycle of the lower stratosphere on day 207. See figure 13 where boxes now show the rate of change of the energy component. Units, —ergs cm^{-2} sec^{-1}.

spread the warming upward and rapidly intensified it.

3) Under the proper conditions, the increasing tropospheric latitudinal temperature gradient with the progress of winter can stimulate high-latitude warmings.

4) The very rapid upper stratospheric polar temperature rise is caused by adiabatic compressional heating and the eddy advection of heat from midlatitudes.

Hirota (1967*a*) investigated the barotropic stability of the polar vortex as it is deformed and elongated under the influence of tropospheric forcing. He found that it became more unstable with increasing deformation and found a tendency for a breakdown of the vortex in the case of deformation in wave number 2. The rapid development of the stratospheric flow into a basically wave-number-2 pattern and the sudden onset of barotropic instability in the upper stratosphere suggests that the same mechanism may be responsible, in part, for this warming.

Working with a highly truncated spectrum consisting of a zonal flow and one wave component, Baer (1968) found that the nonlinear exchange of energy between the zonal flow and the eddy takes place with a definite period. Although these phenomena are not entirely independent, the timing of the warming could be related to a beat effect due to the superposition of the undulating upward flux of kinetic energy and the energy transformation

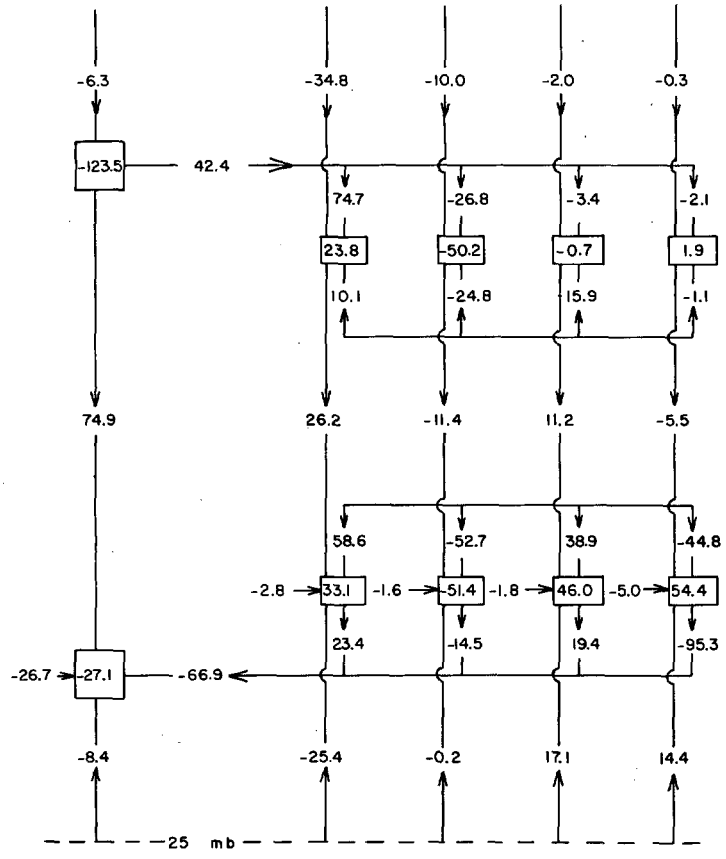

FIGURE 22.—Energy cycle of the upper stratosphere on day 211. See figure 11 for the model where boxes now show the rate of change of the energy component. Units, $-$ergs cm^{-2} sec^{-1}.

$\{K_E \cdot K_Z\}$, whose frequencies are slightly different. An increased upward flux of kinetic energy could enhance the temporary storage of K_Z, and the diminished flux could stimulate the onset of barotropic instability.

5. CONCLUSIONS

There is little doubt that there are some important deficiencies of this simple quasi-geostrophic stratospheric model. Most noteworthy was its inability to produce the observed midlatitude lower stratospheric temperature maximum. This is undoubtedly associated with the poorly defined two-cell mean meridional stratospheric circulation and the weak midlatitude subsiding branch. Manabe and Hunt (1968) found that adiabatic compressional heating in this branch was associated with the temperature maximum. A related problem was the inability of the model to maintain the observed three-cell tropospheric meridional circulation over a long period.

Notwithstanding its shortcomings, the model has been successful in some respects. Starting from the unnatural state of radiative-photochemical equilibrium, a quasi-equilibrium ozone distribution was produced in about 120 days that agreed fairly well with observations. The simple Chapman photochemical theory has been shown to be of practical use, at least for some purposes. The northward transport of ozone from its equatorial source region was accomplished almost exclusively by the planetary scale eddies. The weakness of the meridional circulation and the constraint of considering geostrophic horizontal advection and a constant ozone lapse rate at each level preclude discounting the role of the meridional circulation in the ozone budget.

Rapid radiative-photochemical relaxation of temperature disturbances in the upper stratosphere necessitated upward fluxes of kinetic energy from below to maintain the energy of this region. It is thus important to allow for this relaxation in any model of the upper stratosphere either by treating ozone as an independent variable that freely absorbs solar radiation or by enhancing the infrared Newtonian cooling as done, for instance, by Leovy (1964).

The stratospheric polar vortex was found to be strongly influenced through the interaction of the stratosphere with the troposphere. It was maintained against frictional dissipation by forced eddy momentum fluxes and through upward fluxes of kinetic energy across the tropopause by the meridional circulation.

Nonlinear exchanges of kinetic energy proved to be a vital link in the energetics of the stratosphere, allowing energy to be rapidly transferred from the source region to the sink. Part of the strong upward flux of kinetic energy in wave number 2 across 200 mb was transferred to wave number 1 in the lower stratosphere and then exported to the upper stratosphere to counter the diabatic energy sink. Perry (1967) found nonlinear exchanges to be accomplishing the same purpose in the 1963 warming.

The mere "simulation of a phenomenon does not necessarily imply understanding" (Manabe and Hunt 1968). This is particularly true of the high-latitude warmings in this model. Undoubtedly they were stimulated by augmented forcing from below. The downward-propagating spontaneous warming was associated with an unstable nonlinear reaction of the upper stratosphere to the increased tropospheric forcing. A rapid transfer of kinetic energy up the scale to wave number 1 and the onset of barotropic instability, in the sense that the eddies began transforming zonal to eddy kinetic energy, forced a direct meridional circulation that temporarily heated the Pole through adiabatic compression.

The artificially strengthened tropospheric temperature gradient led to an accelerated baroclinic production of tropospheric kinetic energy prior to the full-scale warming. Increased forcing of the stratosphere across the tropopause drove its initial stage. The sudden onset of barotropic instability in the upper stratosphere rapidly intensified the warming as it spread upward. At the same time, the upper stratosphere became baroclinically unstable, in the sense that zonal available energy was transformed to eddy kinetic energy, and the polar-night jet temporarily weakened in the manner envisaged by Charney and Stern (1962). Nonlinear energy exchanges did not play a vital role in the full-scale warming as they did in the spontaneous warming.

APPENDIX

TABLE 6.—*Spectral data used in radiative-photochemical equilibrium calculations*

Mean wavelength λ	Solar spectral intensity in interval $I_{0\lambda}\Delta\lambda$ Photons $cm^{-2}sec^{-1}$	Ozone absorption cross sections α_3 cm^2 $molecule^{-1}$	α_3' cm^2 $molecule^{-1}$	Oxygen absorption cross section α_2 cm^2 $molecule^{-1}$
7100	2.013×10^{16}	8.04×10^{-22}	1.13×10^{-21}	—
6700	2.092	1.66	2.32	—
6300	2.154	3.39	4.75	—
5900	2.184	4.65	6.51	—
5500	2.148	3.53	4.94	—
5100	2.004	1.59×10^{-21}	2.23×10^{-21}	—
4700	2.030×10^{16}	4.91×10^{-22}	6.87×10^{-22}	—
3400	9.502×10^{14}	9.30×10^{-22}	1.30×10^{-21}	—
3350	9.362×10^{14}	2.01×10^{-21}	2.81	—
3300	9.555	4.65	6.51×10^{-21}	—
3250	8.346	9.68×10^{-21}	1.36×10^{-20}	—
3200	6.848	2.23×10^{-20}	3.12	—
3150	6.503	5.02×10^{-20}	7.03×10^{-20}	—
3100	5.932	1.02×10^{-19}	1.43×10^{-19}	—
3050	5.145	1.94	2.72	—
3000	4.607	3.72	5.21×10^{-19}	—
2950	4.679	7.44×10^{-19}	1.04×10^{-18}	—
2900	3.797	1.41×10^{-18}	1.97	—
2850	2.440	2.49	3.49	—
2800	1.692	3.91	5.47	—
2750	1.523	5.77	8.08×10^{-18}	—
2700	1.699	7.44	1.04×10^{-17}	—
2650	1.334×10^{14}	8.93	1.25	—
2600	9.165×10^{13}	9.86×10^{-18}	1.38	—
2550	7.191	1.04×10^{-17}	1.46	—
2500	4.783	1.02×10^{-17}	1.43	—
2450	4.811×10^{13}	9.30×10^{-18}	1.30	—
2419	9.38×10^{12}	8.50	1.19	4.05×10^{-25}
2400	1.76×10^{13}	7.70	1.08×10^{-17}	6.00×10^{-25}
2375	1.68	7.00	9.80×10^{-18}	1.12×10^{-24}
2350	1.61	6.10	8.54	1.50
2325	1.59	5.40	7.56	1.80
2300	1.51	4.42	6.19	2.18
2275	1.38	3.60	5.04	2.55
2250	1.20	2.90	4.06	3.04
2225	1.01×10^{13}	2.31	3.23	3.68
2200	8.25×10^{12}	1.78	2.49	4.50
2175	6.00	1.35×10^{-18}	1.89	5.17
2150	4.63	9.80×10^{-19}	1.37	6.07
2125	3.40	7.40	1.04×10^{-18}	6.60
2100	2.70	5.40	7.56×10^{-19}	8.00×10^{-24}
2075	2.00	4.05	5.67	1.00×10^{-23}
2050	1.60	3.22	4.51	2.97
2025	1.41	3.01	4.21	2.97
2000	1.28	3.12	4.37	2.97
1975	1.15×10^{12}	3.52	4.93	2.97
1950	9.50×10^{11}	4.00	5.60	7.00
1925	8.25	4.40	6.16	9.30
1900	6.80	4.80	6.72	9.30×10^{-23}
1875	5.75	5.25	7.35	4.46×10^{-22}
1850	4.75	5.70	7.98	1.86×10^{-21}
1825	3.80	6.20	8.68	9.00×10^{-21}
1806	1.60×10^{11}	6.70×10^{-19}	9.38×10^{-19}	4.46×10^{-20}

ACKNOWLEDGMENTS

The author is grateful to Dr. Richard A. Craig for his encouragement and helpful suggestions. Thanks are also due Doctors Bernhard Haurwitz and Robert E. Dickinson for critically reviewing the manuscript.

Financial support was provided by the Air Force Cambridge Research Laboratories under Contract F19628-68-C-0112 and the National Science Foundation under Grant GA333. All computations were performed at the Florida State University Computing Center and the cost, in part, paid by the National Science Foundation under Grant GP5114.

REFERENCES

Baer, F., "Studies in Low-Order Spectral Systems," *Atmospheric Sciences Paper* No. 129, Department of Atmospheric Sciences, Colorado State University, Fort Collins, **1968**, 77 pp.

Batten, E. S., "Wind Systems in the Mesosphere and Lower Ionosphere," *Journal of Meteorology*, Vol. 18, No. 3, June **1961**, pp. 283–291.

Benson, S. W., and Axworthy, A. E., Jr., "Mechanism of the Gas Phase, Thermal Decomposition of Ozone," *Journal of Chemical Physics*, Vol. 26, No. 6, June **1957**, pp. 1718–1726.

Berkofsky, L., and Bertoni, E. A., "Mean Topographic Charts for the Entire Earth," *Bulletin of the American Meteorological Society*, Vol. 36, No. 7, Sept. **1955**, pp. 350–354.

Brewer, A. W., and Wilson, A. W., "Measurements of Solar Ultraviolet Radiation in the Stratosphere," *Quarterly Journal of the Royal Meteorological Society*, Vol. 91, No. 390, Oct. **1965**, pp. 452–461.

Bryan, Kirk, Jr., "A Numerical Investigation of Certain Features of the General Circulation," *Tellus*, Vol. 11, No. 2, May **1959**, pp. 163–174.

Burger, A. P., "Scale Consideration of Planetary Motions of the Atmosphere," *Tellus*, Vol. 10, No. 2, May **1958**, pp. 195–205.

Byron-Scott, R., "A Stratospheric General Circulation Experiment Incorporating Diabatic Heating and Ozone Photochemistry," *Publication in Meteorology* No. 87, Arctic Meteorology Research Group, Department of Meteorology, McGill University, Montreal, Quebec, Apr. **1967**, 201 pp. plus appendices.

Chapman, S., "A Theory of Upper-Atmospheric Ozone," *Memoirs of the Royal Meteorological Society*, Vol. 3, No. 26, June **1930**, pp. 103–125.

Charney, Jule G., "On the Theory of the General Circulation of the Atmosphere," *The Atmosphere and the Sea in Motion*, Rockefeller Institute Press, New York, **1959**, pp. 178–193.

Charney, Jule G., and Eliassen, Arnt, "A Numerical Method for Predicting the Perturbations of the Middle-Latitude Westerlies," *Tellus*, Vol. 1, No. 2, May **1949**, pp. 38–44.

Charney, Jule G., and Stern, M. E., "On the Stability of Internal Baroclinic Jets in a Rotating Atmosphere," *Journal of the Atmospheric Sciences*, Vol. 19, No. 2, Mar. **1962**, pp. 159–172.

Clark, J. H. E., "A Spectral Model of the Winter Stratosphere," *Scientific Report* No. 69–7, Department of Meteorology, Fiorida State University, Tallahassee, **1969**, 155 pp.

Craig, R. A., "The Observations and Photochemistry of Atmospheric Ozone and Their Meteorological Significance," *Meteorological Monograms*, Vol. 1, No. 2, American Meteorological Society, Boston, Mass., Sept. **1950**, 50 pp.

Craig, R. A., *The Upper Atmosphere: Meteorology and Physics*, Academic Press, New York, **1965**, 509 pp.

Craig, R. A., "The Vorticity Budget of the Wintertime Lower Stratosphere," *Journal of the Atmospheric Sciences*, Vol. 24, No. 5, Sept. **1967**, pp. 558–568.

Craig, R. A., and Lateef, M. A., "Vertical Motion During the 1957 Stratospheric Warming," *Journal of Geophysical Research*, Vol. 67, No. 5, May 1962, pp. 1839–1854.

Deland, Raymond J., "On the Scale Analysis of Traveling Planetary Waves," *Tellus*, Vol. 17, No. 4, Nov. **1965**, pp. 527–528.

Dickinson, Robert E., "A Note on Geostrophic Scale Analysis of Planetary Waves," *Tellus*, Vol. 20, No. 3, Aug. **1968**, pp. 548–550.

Dütsch, Hans U., "Current Problems of the Photochemical Theory of Atmospheric Ozone," *Chemical Reactions in the Lower and Upper Atmosphere*, Interscience Publishers, New York, **1961**, 390 pp. (see pp. 167–180).

Environmental Science Services Administration, National Aeronautics and Space Administration, and U.S. Air Force, *U.S. Standard Atmosphere Supplements, 1966*, Washington, D.C., **1967**, 289 pp.

Finger, Frederick G., and Teweles, Sidney, "The Mid-Winter 1963 Stratospheric Warming and Circulation Change," *Journal of Applied Meteorology*, Vol. 3, No. 1, Feb. **1964**, pp. 1–15.

Godson, W. L., "Total Ozone and the Middle Stratosphere Over Arctic and Sub-Arctic Areas in Winter and Spring," *Quarterly Journal of the Royal Meteorological Society*, Vol. 86, No. 369, July **1960**, pp. 301–317.

Henrici, P., *Elements of Numerical Analysis*, John Wiley & Sons, Inc., New York, **1964**, 328 pp.

Hering, W. S., and Borden, T. R., Jr., "Ozonesonde Observations Over North America, Volume 2," *Environmental Research Papers* No. 38, U.S. Air Force Cambridge Research Laboratories, Hanscom Field, Mass., July **1964**, 280 pp.

Hering, W. S., Touart, C. N., and Borden, T. R., Jr., "Ozone Heating and Radiative Equilibrium in the Lower Stratosphere," *Journal of the Atmospheric Sciences*, Vol. 24, No. 4, July **1967**, pp. 402–413.

Hirota, Isamu, "Dynamic Instability of Stratospheric Polar Vortex," *Journal of the Meteorological Society of Japan*, Vol. 45, No. 5, Oct. **1967***a*, pp. 409–421.

Hirota, Isamu, "The Vertical Structure of the Stratospheric Sudden Warming," *Journal of the Meteorological Society of Japan*, Vol. 45, No. 5, Oct. **1967***b*, pp. 422–435.

Hunt, Barrie G., "Photochemistry of Ozone in a Moist Atmosphere," *Journal of Geophysical Research*, Vol. 71, No. 5, Mar. **1966**, pp. 1385–1398.

Hunt, Barrie G., "Experiments With a Stratospheric General Circulation Model: III. Large-Scale Diffusion of Ozone Including Photochemistry," *Monthly Weather Review*, Vol. 97, No. 4, Apr. **1969**, pp. 287–306.

Hunt, Barrie G., and Manabe, Syukuro, "Experiments With a Stratospheric General Circulation Model: II. Large-Scale Diffusion of Tracers in the Stratosphere," *Monthly Weather Review*, Vol. 96, No. 8, Aug. **1968**, pp. 503–539.

Kuo, H.-L., "Forced and Free Meridional Circulation in the Atmosphere," *Journal of Meteorology*, Vol. 13, No. 6, Dec. **1956**, pp. 561–568.

Leovy, Conway, "Simple Models of Thermally Driven Mesopheric Circulations," *Journal of the Atmospheric Sciences*, Vol. 21, No. 4, July **1964**, pp. 327–341.

Lindzen, Richard S., "The Radiative-Photochemical Response of the Mesosphere to Fluctuations in Radiation," *Journal of the Atmospheric Sciences*, Vol. 22, No. 5, Sept. **1965**, pp. 469–478.

Lindzen, Richard S., Department of Geophysical Sciences, University of Chicago, **1969** (personal communication).

Lindzen, Richard S., and Goody, Richard, "Radiative and Photochemical Processes in Mesospheric Dynamics: Part I, Models for Radiative and Photochemical Processes," *Journal of the Atmospheric Sciences*, Vol. 22, No. 4, July **1965**, pp. 341–348.

London, J., and Prabhakara, C., "The Effect of Stratospheric Transport Processes on the Ozone Distribution," *Scientific Report* No. 8, U.S. Air Force Cambridge Research Laboratories, Hanscom Field, Mass., **1964**, 19 pp.

Lorenz, Edward N., "Energy and Numerical Weather Prediction," *Tellus*, Vol. 12, No. 4, Nov. **1960**, pp. 364–373.

Mahlman, J. D., "Energetics of a 'Minor Breakdown' of the Stratospheric Polar Night Vortex," *Journal of the Atmospheric Sciences*, Vol. 26, No. 6, Nov. **1969**, pp. 1306–1317.

Manabe, Syukuro, and Hunt, Barrie G., "Experiments With a Stratospheric General Circulation Model: I. Radiative and Dynamic Aspects," *Monthly Weather Review*, Vol. 96, No. 8, Aug. **1968**, pp. 477–502.

Manabe, Syukuro, and Möller, Fritz, "On the Radiative Equilibrium and Heat Balance of the Atmosphere," *Monthly Weather Review*, Vol. 89, No. 12, Dec. **1961**, pp. 503–532.

Muench, H.S., "On the Dynamics of the Wintertime Stratosphere Circulation, "*Journal of the Atmospheric Sciences*, Vol. 22, No. 4, July **1965**, pp. 349–360.

Murray, F. W., "Dynamic Stability in the Stratosphere," *Journal of Geophysical Research*, Vol. 65, No. 10, Oct. **1960**, pp. 3273–3305.

Newell, R. E., "Transfer Through the Tropopause and Within the Stratosphere," *Quarterly Journal of the Royal Meteorological Society*, Vol. 89, No. 380, Apr. **1963**, pp. 167–204.

Oort, Abraham H., "On the Energetics of the Mean and Eddy Circulations in the Lower Stratosphere," *Tellus*, Vol. 16, No. 4, Nov. **1964**, pp. 309–327.

Peng, L., "A Simple Numerical Experiment Concerning the General Circulation in the Lower Stratosphere, "*Pure and Applied Geophysics*, Vol. 61, No. 2, May **1965**, pp. 191–218.

Perry, J. S., "Long-Wave Energy Processes in the 1963 Sudden Stratospheric Warming," *Journal of the Atmospheric Sciences*, Vol. 24, No. 5, Sept. **1967**, pp. 539–550.

Platzman, G. W., "The Spectral Form of the Vorticity Equation," *Journal of Meteorology*, Vol. 17, No. 6, Dec. **1960**, pp. 835–844.

Prabhakara, Cuddapah, "Effects of Non-Photochemical Processes on the Meridional Distribution and Total Amount of Ozone in the Atmosphere," *Monthly Weather Review*, Vol. 91, No. 9, Sept. **1963**, pp. 411–431.

Reed, R. J., Wolfe, J. L., and Nishimoto, H., "A Spectral Analysis of the Energetics of the Stratospheric Sudden Warming of Early 1957," *Journal of the Atmospheric Sciences*, Vol. 20, No. 4, July **1963**, pp. 256–275.

Saltzman, Barry, "On the Theory of Winter-Average Perturbations in the Troposphere and Stratosphere," *Monthly Weather Review*, Vol. 93, No. 4, Apr. **1965**, pp. 195–211.

Saltzman, Barry, and Teweles, Sidney, "Further Statistics on the Exchange of Kinetic Energy Between Harmonic Components of the Atmospheric Flow," *Tellus*, Vol. 16, No. 4, Nov. **1964**, pp. 432–435.

Scherhag, Richard, "Die Explosionsortigen Stratosphärenerwarmungen des Spätwinters 1951/52" (The Explosionlike Stratospheric Warmings of the Late Winter 1951/52), *Berichte der Deutschen Wetterdienstes U.S. Zone*, No. 38, Bad Kissingen, Deutscher, Jan. **1952**, pp. 51–63.

Silberman, I., "Planetary Waves in the Atmosphere," *Journal of Meteorology*, Vol. 11, No. 1, Feb. **1954**, pp. 27–34.

Smagorinsky, Joseph, Manabe, Syukuro, and Holloway, J. Leith, Jr., "Numerical Results From a Nine-Level General Circulation Model of the Atmosphere," *Monthly Weather Review*, Vol. 93, No. 12, Dec. **1965**, pp. 727–768.

Starr, Victor P., "Questions Concerning the Energy of Stratospheric Motions," *Archiv für Meteorologie, Geophysik und Bioklimatologie, Ser. A: Meteorologie und Geophysik*, Vol. 12, No. 1, Jan. **1960**, pp. 1–7.

Teweles, Sidney, "Spectral Aspects of the Stratospheric Circulation During the IGY, "*Planetary Circulations Project, Report* No. 8, Massachusetts Institute of Technology Press, Cambridge, Jan. **1963**, 191 pp.

[*Received October 2, 1969; revised December 24, 1969*]